NASA TECHNICAL NOTE

NASA TN D-4853

NASA TN D-4853

USE OF BARONTI-LIBBY TRANSFORMATION AND PRESTON TUBE CALIBRATIONS TO DETERMINE SKIN FRICTION FROM TURBULENT VELOCITY PROFILES

by Jerry M. Allen

Langley Research Center
Langley Station, Hampton, Va.

NATIONAL AERONAUTICS AND SPACE ADMINISTRATION • WASHINGTON, D. C. • NOVEMBER 1968

USE OF BARONTI-LIBBY TRANSFORMATION AND PRESTON TUBE CALIBRATIONS TO DETERMINE SKIN FRICTION FROM TURBULENT VELOCITY PROFILES

By Jerry M. Allen

Langley Research Center
Langley Station, Hampton, Va.

NATIONAL AERONAUTICS AND SPACE ADMINISTRATION

For sale by the Clearinghouse for Federal Scientific and Technical Information
Springfield, Virginia 22151 – CFSTI price $3.00

USE OF BARONTI-LIBBY TRANSFORMATION AND PRESTON TUBE CALIBRATIONS TO DETERMINE SKIN FRICTION FROM TURBULENT VELOCITY PROFILES

By Jerry M. Allen
Langley Research Center

SUMMARY

A large number of velocity profiles with corresponding local skin-friction measurements have been used to investigate the validity of the Baronti-Libby transformation as a skin-friction measuring technique over a wide range of test conditions. The possibility of using existing Preston tube calibrations to calculate skin friction from velocity profiles is investigated, and a computational procedure is developed so that a Clauser-type determination of skin friction from velocity profiles can be accomplished without the necessity of plotting.

The principal conclusions that result from this study are that the Baronti-Libby transformation gives good results for adiabatic flow but does not predict the correct trend with heat transfer and that using the Fenter-Stalmach law only as a Preston tube calibration is unduly restrictive since it is shown that the law can be used to calculate local skin friction from conventional velocity profiles with results that are comparable with those of the more complex Baronti-Libby method.

INTRODUCTION

The most practical result of the development of the law of the wall velocity profile theory for incompressible, turbulent flow by Prandtl in the 1920's is that it permits calculation of local skin friction from impact pressure measurements. (See appendix (eqs. (A4) and (A5)) for the incompressible law of the wall equations.) The use of this theory in succeeding decades has resulted in two distinctly different applications:

(1) Graphical interpolation of skin friction from experimental velocity profiles in the manner first proposed by Clauser (ref. 1) in 1954, and (2) calculation of skin friction from experimental impact pressure measurements with large round probes resting on the test surface, commonly called Preston tubes.

The use of Prandtl's concept in supersonic flow awaited the development of compressible law of the wall theory. In 1957, Fenter and Stalmach (ref. 2) derived a

compressible law of the wall theory but used it only as a Preston tube calibration and not for the determination of skin friction from velocity profiles. Recently, Baronti and Libby (ref. 3), following the work of Coles (ref. 4), transformed the incompressible law of the wall to compressible flow and used the resulting equations to determine skin friction from compressible velocity profiles.

In recent Preston tube work, Hopkins and Keener (ref. 5) experimentally obtained a supersonic calibration which is stated to give results which are close to those obtained from the Fenter-Stalmach law (within approximately 5 percent). Sigalla (ref. 6) proposed that the reference enthalpy concept be applied to the incompressible Preston tube calibration, and thereby make it valid for compressible flow.

This paper has three basic objectives. The first is to check the validity of the Baronti-Libby transformation by amassing available data in which both velocity profiles and local skin friction were measured for the same test conditions. The skin friction determined by the Baronti-Libby technique is then compared with the measured skin friction.

The second objective is to investigate the possibility of using Preston tube calibrations to determine skin friction from velocity profiles. These calibrations are intended to calculate local skin friction from the pressure measurements of large round impact probes resting on the test surface. In some calibrations this pressure is converted to velocity or Mach number (called probe velocity and probe Mach number, respectively). Basically, however, these Preston tube calibrations are derived from law of the wall theory; thus, their use only with Preston probes might be unduly restrictive. This second objective, therefore, is accomplished by using the three compressible Preston tube calibrations mentioned – Fenter-Stalmach, Hopkins-Keener, and Sigalla – to calculate skin-friction coefficients from velocity profiles in the manner of Clauser and to compare the results with those of experimental measurements.

The last objective is to demonstrate how a Clauser-type determination of skin friction from experimental velocity profiles can be accomplished analytically without the necessity of plotting each profile and interpolating the answer.

The experimental data used in this study were gathered from nine sources which contained a total of 167 velocity profiles with accompanying experimental skin-friction measurements. Most of these measurements were made by skin-friction balances, but a few were obtained from heat-transfer data and velocity slopes at the wall.

SYMBOLS

C_f	local skin-friction coefficient, $\frac{\tau_w}{\frac{1}{2}\rho_e U_e^2}$
d	impact probe diameter
M	Mach number
R	unit Reynolds number, $\frac{\rho_e U_e}{\mu_e}$
R_d	Reynolds number based on tube diameter, $\frac{\rho_e U_e d}{\mu_e}$
R_y	Reynolds number based on normal coordinate, $\frac{\rho_e U_e y}{\mu_e}$
R_θ	Reynolds number based on momentum thickness $\frac{\rho_e U_e \theta}{\mu_e}$
T	absolute temperature
U	velocity in streamwise direction
y	normal coordinate
δ	boundary-layer thickness
θ	boundary-layer momentum thickness, $\int_0^\delta \frac{\rho U}{\rho_e U_e}\left(1 - \frac{U}{U_e}\right)dy$
μ	absolute viscosity
ζ	normal coordinate in law of the wall profile, $\frac{y\rho}{\mu}\sqrt{\frac{\tau_w}{\rho_w}}$
γ	ratio of specific heats
ρ	density
σ	scaling parameter in Baronti-Libby transformation theory
τ	shearing stress

Subscripts:

aw	adiabatic wall conditions
e	edge of boundary-layer conditions
f	edge of laminar sublayer conditions
t	free-stream stagnation conditions
w	wall conditions

Bars over symbols denote transformed quantities. Primes denote quantities evaluated at reference temperature.

DETERMINATION OF C_f BY BARONTI-LIBBY METHOD

Technique

Perhaps the most useful aspect of the Baronti-Libby transformation (ref. 3) of compressible velocity profiles to incompressible form is that local skin friction can be determined from the profiles in a manner similar to that first proposed by Clauser (ref. 1) for incompressible flow. Experimental verification of this method is needed, however, before it can be used with confidence as a skin-friction measuring technique. Baronti and Libby compared, with encouraging results, the skin-friction coefficients calculated by this technique with those measured with skin-friction balances. The amount of data used in this comparison, however, was small compared with the total amount of data available.

In the present study an attempt was made to gather available data in which both velocity profiles and experimental skin-friction measurements were made. A total of 167 profiles was found; 138 were for adiabatic wall conditions in which skin-friction balance measurements were made $(M_e < 5)$, and 29 were for nonadiabatic wall conditions $(5 < M_e < 8)$ in which local skin friction was determined either from heat-transfer measurements or from velocity profile slope at the wall. This study is restricted to profiles obtained in air on flat surfaces in compressible flow. It should be noted that profiles 1 to 5 (see table I) were obtained by private communications with Messrs. Hopkins and Keener, and are not included in reference 5 although some results derived from these profiles are presented. The other profiles in table I were obtained from references 7 to 14.

The usual method of using the Baronti-Libby transformation consists of plotting experimental velocity profiles in the form of U/U_e against $R\int_0^y \frac{\rho}{\rho_e}\,dy$ and calculating

curves of constant $\overline{C}_f$ from the theory. (See appendix.) By comparing the theory curves with the data, the value of $\overline{C}_f$ which best fits the data in the law of the wall region can be interpolated, and from this C_f can be calculated. A sample profile using this technique (fig. 1) shows that the region of constant skin friction is easily detectable. The reason that the constant skin-friction region does not extend completely through the lower part of the boundary layer is probably due to probe-wall interference effects near the test surface together with the assumed constant total temperature through the boundary layer.

This technique is difficult and tedious to use when a large number of profiles are involved, since it requires plotting, integration of the experimental data, and different theory curves for each free-stream Mach number. For this reason an analytic method was developed for this study so that the plotting requirements for using the Baronti-Libby transformation would be eliminated. The Baronti-Libby equations, given in the appendix, were programed on a digital computer so that the skin friction of each data point in the profile could be easily calculated. The wall skin friction was then selected from the range of data where the values of skin friction remained fairly constant. It should be noted that the technique used in this paper determines C_f only from the logarithmic portion of the boundary layer, and not from the laminar sublayer. As Mach number increases, the laminar sublayer becomes a larger part of the boundary layer. Also, as Reynolds number decreases, the upper limit of the logarithmic portion of the boundary layer decreases. Profiles taken at conditions of high Mach number and low Reynolds number would contain a law of the wall region composed entirely of sublayer, and therefore could not be used by the technique developed in this paper. Under normal test Reynolds numbers, however, this technique should be good throughout the supersonic and low hypersonic Mach number range.

As an example of this technique, the velocity profile previously shown in figure 1 is given in table II along with the machine-computed values of $\overline{C}_f$ and C_f.

Comparison With Experiment

The skin-friction results of this procedure (fig. 2) for adiabatic profiles scatter approximately ± 5 percent about the line of perfect agreement. These results, along with others to be discussed later in this paper, are listed in table I.

DETERMINATION OF C_f BY PRESTON TUBE CALIBRATIONS

Technique

Although the Baronti-Libby method gives good results over a wide range of test conditions, it is difficult to use without computer help because of the lengthy and tedious calculations involved. An alternate procedure to the Baronti-Libby method is proposed in

this paper – the use of Preston tube calibrations to calculate skin friction from velocity profiles in a manner similar to the law of the wall technique.

The reason this approach was tried is that basically Preston tube calibrations are derived from law of the wall theory. The difference between the two is that in Preston tube calibrations, one of the law of the wall variables y is replaced by $d/2$, and this law is then used with round probes in contact with the test surface. Hence, the variables τ_w, U/U_e, and y of law of the wall theory are replaced by τ_w, U/U_e, and d in Preston tube calibrations. (In some calibrations, pressure or Mach number ratio is used instead of velocity ratio.)

It seems logical, therefore, that if the original variable y were inserted in the Preston tube calibrations in the place of $d/2$, this calibration could be used not only with measurements from round impact probes in contact with the test surface, but also with conventional velocity profile measurements in which flattened impact probes were used. The Preston tube calibrations used in this study calculate local skin friction from measurements made in the logarithmic portion of the boundary layer. Therefore the same cautionary remark about high Mach number, low Reynolds number boundary layers given earlier in connection with the Baronti-Libby transformation is applicable here.

Three Preston tube calibrations were converted in the manner described – Fenter-Stalmach (ref. 2), Hopkins-Keener (ref. 5), and Sigalla (ref. 6). The equations are given in the appendix. Since the variables are now τ_w, y, and U/U_e (or M/M_e in the case of Hopkins-Keener), plots could be made of U/U_e (or M/M_e) as a function of R_y with C_f as a parameter. Plotting experimental data on these coordinates would yield the correct C_f in the same manner that Clauser first proposed for incompressible flow. Figure 3 shows the profile that was used in the Baronti-Libby sample plot along with the three Preston tube laws. It can be seen that the region of constant skin friction is easy to distinguish for all three laws; the interpolation of C_f by this method is thus allowed.

Figure 3(b) shows a characteristic which was noticed in many of the profiles used in this study – which is that the Sigalla calibration appears to be skewed relative to the data. This skewness results in the region of constant skin friction occurring at very high values of velocity ratio – 0.88 to 0.98, approximately. Some of the profiles, in fact, were so skewed that no constant skin-friction region could be found, even at the high velocity ratios. Since these high velocity ratios are above the range of the law of the wall, much of the agreement (presented later in this paper) between the measured skin-friction values and those calculated from the Sigalla calibration is probably fortuitous.

Notice that the Hopkins-Keener sample plot (fig. 3(c)) shows a much larger number of data points with approximately constant C_f than is shown in the other methods. The effect is partly due to the Hopkins-Keener calibration using Mach number ratio as a parameter which requires no assumption about total temperature through the boundary

layer. The other laws, on the other hand, use velocity ratio which, for adiabatic flows, is usually calculated from the Mach number ratio by assuming a total temperature distribution through the boundary layer which is constant and equal to the boundary-layer edge value. This assumption, of course, becomes progressively worse as the wall is approached (that is, decreasing R_y).

It should be noted that the sample profile used to illustrate this technique contains many more data points than are needed for this method. Unlike the Baronti-Libby transformation, these Preston tube calibrations require no integration of experimental data, and thereby detailed profiles are unnecessary.

The computational procedure for C_f described in the Baronti-Libby section of this paper was used with the three Preston tube calibrations so that the necessity of plotting all the profiles in this study would be eliminated. Table III lists the calculated values of skin friction for the same sample profile shown earlier.

Comparison With Experiment

Figure 4 shows a comparison between the local skin friction calculated from the Fenter-Stalmach calibration and measured local skin friction. The profiles and experimental C_f used here are the same as those used in the Baronti-Libby correlation shown earlier. The comparison between calculated and measured C_f can be seen to be very good, the scatter being of the same order that was present in the Baronti-Libby correlation.

The values of C_f calculated from the Sigalla calibration are shown in figure 5. The scatter here is somewhat larger than was seen in the Baronti-Libby or Fenter-Stalmach figures. Most of the large scatter, however, results from only one set of data, although there are a large number of profiles in this set. It should be noted at this point that much of the Sigalla agreement is probably fortuitous because of the Sigalla C_f values being obtained outside of the law of the wall region, as discussed earlier. Figure 6 shows the data from the profiles calculated by the Hopkins-Keener calibration compared with the measured data. The scatter here is much larger than that of the other methods and had a definite bias in the direction of higher calculated skin friction. By plotting these data as a function of Mach number (fig. 7), it can be seen that there is a definite Mach number trend in the Hopkins-Keener results. It should be noted that the results presented in this section were obtained from the Preston tube laws directly as they appear in the respective references, and no attempt was made to modify the calibrations. For example, the power-law viscosity-temperature relationship (see eq. (A20)) was used in the Fenter-Stalmach law instead of the more accurate Sutherland viscosity law. Also, the Hopkins-Keener calibration was not modified in an attempt to eliminate probe displacement effects. The calibration, as given by equation (A23), collapses compressible

Preston tube data to the Preston incompressible curve. Velocity profiles, however, being obtained with impact probes which are very small compared with the boundary-layer thickness, have negligible probe displacement effects. A more appropriate curve on which to correlate supersonic velocity profile data, therefore, would be Coles curve, which contains zero displacement effects. (See fig. 5(a) of ref. 5 for a comparison between the two curves.) The difference between these two incompressible curves – that is, Preston and Coles – represents approximately 5 percent in skin friction. If the Coles curve had been used as the incompressible base instead of the Preston curve, all the Hopkins-Keener C_f data of figures 6 and 7 would have been about 5 percent lower. Since the scatter in the data and its trend with Mach number would not have changed, the general conclusions derived from this study of the Hopkins-Keener calibration are not affected.

The fact that different results were obtained from the Fenter-Stalmach and Hopkins-Keener methods seems contradictory since Hopkins and Keener report in reference 5 that the two calibrations are in close agreement in the linear part of the curves – the only part used in this study. The difference between the two is given to be the same order as the differences between the Preston and Coles incompressible curves – that is, approximately 5 percent. The basis on which this conclusion was drawn, however, was that the Hopkins-Keener Preston tube data, on which their calibration was based, agreed with the Fenter-Stalmach calibration and conversely that the Fenter-Stalmach data agreed with the Hopkins-Keener calibration. No direct comparison was made, however, between the two calibrations.

Figure 8 shows how the two calibrations compare over a wide range of test conditions. It can be seen that the calibrations give identical results only for values of probe velocity ratio of about 0.6. The Hopkins-Keener Preston tube data contained velocity ratios which were sufficiently close to this value that similar results were obtained with the two calibrations. The law of the wall region, however, covers a much wider range of velocity ratios. For the profiles used in this study, the maximum extent of this region ranged from about $U/U_e \approx 0.6$ to $U/U_e \approx 0.9$, depending on the test conditions. Figure 8 shows that the skin-friction coefficients calculated by the two calibrations are increasingly divergent with increasing values of U/U_e. It also explains the Mach number trend in the results calculated from the Hopkins-Keener calibration.

COMPARISON BETWEEN BARONTI-LIBBY AND FENTER-STALMACH LAWS

A direct comparison between the Baronti-Libby and Fenter-Stalmach results for the adiabatic profiles used earlier is shown in figure 9. The agreement between the two is seen to be very good – better, in fact, than the agreement of each method with measured skin friction as shown in figures 2 and 4. It is recommended, therefore, for the range of test conditions represented in figure 9 ($1.6 < M_e < 4.6$; $0.02 \times 10^6 < R/cm < 1.14 \times 10^6$;

$2 \times 10^3 < R_\theta < 7 \times 10^5$, and $294 < T_t$, $^oK < 339$), that the Fenter-Stalmach Preston tube calibration used in the manner described in this paper be considered as a satisfactory alternative to the more complex Baronti-Libby method for determining skin friction from velocity profiles.

EFFECT OF HEAT TRANSFER ON BARONTI-LIBBY AND FENTER-STALMACH RESULTS

All the results presented thus far have been for adiabatic test conditions, for which there are much data available. There are much less data, however, taken under conditions of heat transfer, and those that are available (refs. 8 and 9) do not contain direct skin-friction measurements, but calculated skin friction from velocity profile slope at the wall and heat-transfer measurements. Hence the cold wall results presented below probably contain more uncertainties than are contained in the adiabatic wall results presented earlier. It is reassuring to note, however, that results similar to those reported below were obtained by Bertram, et al. (ref. 15) who compared Baronti-Libby skin-friction results with those calculated by the Spalding and Chi technique (see ref. 16), and those measured in a few cases.

Neither the Baronti-Libby nor Fenter-Stalmach methods appear to give good results under conditions of large heat transfer, as can be seen from figures 10 and 11. These figures show a definite bias in the direction of higher skin friction and that the bias grows larger with decreasing wall temperature ratio.

It is interesting to note that better results are obtained if the profiles used are assumed to be adiabatic. This assumption, in general, results in lower skin friction for the cold walls profiles and, therefore, better agreement with the experimental values as can be seen in figures 12 and 13. There is a very noticeable improvement in the Fenter-Stalmach results (fig. 13), whereas the improvement in the Baronti-Libby results is somewhat less (fig. 12).

CONCLUSIONS

Based on the results of a study of a large number of two-dimensional, zero-pressure gradient, compressible velocity profiles with corresponding experimental skin-friction measurements, the following conclusions are made:

1. The Baronti-Libby method of determining local skin friction from velocity profiles gives good results for adiabatic flow but does not predict the correct trend with heat transfer.

2. Using the Fenter-Stalmach law of the wall only as a Preston tube calibration is unduly restrictive since it is shown in this paper that the law can be used to obtain local skin friction from conventional velocity profiles with results that are comparable with those of the more complex Baronti-Libby method. Of all the Preston tube calibrations evaluated, the Fenter-Stalmach law gave the best results.

3. It has been shown in this paper that a Clauser-type determination of local skin friction from experimental velocity profiles can be accomplished analytically without the necessity of plotting each profile and interpolating the answer.

Langley Research Center,
National Aeronautics and Space Administration,
Langley Station, Hampton, Va., June 14, 1968,
720-01-00-17-23.

APPENDIX

SKIN-FRICTION EQUATIONS

The equations used in this study to calculate skin friction from velocity profiles are derived in this appendix. The equations for the Baronti-Libby transformation and the Preston tube calibrations of Fenter-Stalmach, Hopkins-Keener, and Sigalla are put in a form so that the skin friction is calculated from profiles in the form of y and U/U_e, the flow conditions being given by M_e, R, T_t, and T_w/T_e.

Baronti-Libby Equations

Baronti and Libby (ref. 3) give the following equations for transforming the compressible law of the wall to the incompressible form

$$\bar{\zeta} = \sqrt{\frac{\bar{C}_f}{2}}\left(\frac{\mu_e \sigma}{\bar{\mu}}\right) R \int_0^y \frac{\rho}{\rho_e}\, dy \tag{A1}$$

$$C_f = \frac{\rho_w \mu_w}{\rho_e \mu_e}\left(\frac{\sigma \mu_e}{\bar{\mu}}\right)\bar{C}_f \tag{A2}$$

and

$$\frac{U}{U_e} = \frac{\bar{U}}{\bar{U}_e} \tag{A3}$$

These equations are used with the incompressible law of the wall, which is given as

$$\frac{\bar{U}}{\bar{U}_e} = \sqrt{\frac{\bar{C}_f}{2}}\, f(\bar{\zeta}) \tag{A4}$$

where

$$\left.\begin{aligned} f(\bar{\zeta}) &= \bar{\zeta} && \left(0 \leq \bar{\zeta} < \bar{\zeta}_f\right) \\ f(\bar{\zeta}) &= 2.43 \log_e 7.5\bar{\zeta} && \left(\bar{\zeta}_f < \bar{\zeta} < \bar{\zeta}_1\right) \end{aligned}\right\} \tag{A5}$$

The limits $\bar{\zeta}_f$ and $\bar{\zeta}_1$ are the values of $\bar{\zeta}$ at the edge of the laminar sublayer and the outer limit of the region of applicability of the law of the wall, respectively.

The skin friction is determined in this paper only from the logarithmic portion of the boundary layer; hence, equation (A5) may be written as

$$f(\bar{\zeta}) = 2.43 \log_e 7.5\bar{\zeta} \tag{A6}$$

Substituting equations (A6), (A1), and (A3) into equation (A4) gives

$$\frac{U}{U_e} = \sqrt{\frac{\overline{C_f}}{2}}\, 2.43 \log_e\left[7.5\sqrt{\frac{\overline{C_f}}{2}}\left(\frac{\mu_e \sigma}{\overline{\mu}}\right) R \int_0^y \frac{\rho}{\rho_e}\, dy\right] \tag{A7}$$

The density distribution is assumed by Baronti and Libby as

$$\frac{\rho_e}{\rho} = \frac{T_w}{T_e} + \left(1 + \frac{\gamma - 1}{2} M_e^2 - \frac{T_w}{T_e}\right)\frac{U}{U_e} - \frac{\gamma - 1}{2} M_e^2 \left(\frac{U}{U_e}\right)^2 \tag{A8}$$

Assuming $\gamma = 1.4$ results in

$$\frac{\rho_e}{\rho} = \frac{T_w}{T_e} + \left(1 + 0.2\, M_e^2 - \frac{T_w}{T_e}\right)\frac{U}{U_e} - 0.2\, M_e^2 \left(\frac{U}{U_e}\right)^2 \tag{A9}$$

Substituting equation (A9) into equation (A7) yields

$$\frac{U}{U_e} = 1.718\sqrt{\overline{C_f}} \log_e\left\{5.3\sqrt{\overline{C_f}}\left(\frac{\sigma\mu_e}{\overline{\mu}}\right) R \int_0^y \left[\frac{T_w}{T_e} + \left(1 + 0.2\, M_e^2 - \frac{T_w}{T_e}\right)\frac{U}{U_e} - 0.2\, M_e^2 \left(\frac{U}{U_e}\right)^2\right]^{-1} dy\right\} \tag{A10}$$

The integrand in equation (A10) is evaluated at each point in the profile and the integration is performed by parabolic curve fits.

Assuming constant static pressure through the boundary layer and Sutherland's viscosity law results in

$$\frac{\rho_w \mu_w}{\rho_e \mu_e} = \sqrt{\frac{T_w}{T_e}}\, \frac{T_t + 199 + 39.8\, M_e^2}{\frac{T_w}{T_e} T_t + 199 + 39.8\, M_e^2} \tag{A11}$$

Hence, equation (A2) may be written as

$$C_f = \sqrt{\frac{T_w}{T_e}}\, \frac{T_t + 199 + 39.8\, M_e^2}{\frac{T_w}{T_e} T_t + 199 + 39.8\, M_e^2}\, \frac{\sigma\mu_e}{\overline{\mu}}\, \overline{C_f} \tag{A12}$$

The parameter $\frac{\sigma\mu_e}{\overline{\mu}}$ is given by Baronti and Libby to be

$$\frac{\sigma\mu_e}{\overline{\mu}} = \frac{\rho_f}{\rho_e}\frac{\mu_e}{\mu_f}\, \overline{\zeta}_f^{-1} \int_0^{\overline{\zeta}_f} \frac{\rho_e}{\rho}\, d\overline{\zeta} \tag{A13}$$

Again assuming constant static pressure through the boundary layer and Sutherland's viscosity law, and taking $\overline{\zeta}_f$ to be 10.6 as given by Clauser and used by Baronti and Libby yields, after performing the required integration,

APPENDIX

$$\frac{\sigma\mu_e}{\bar{\mu}} = \frac{\left[\frac{T_w}{T_e} T_t + \left(1 + 0.2M_e^2 - \frac{T_w}{T_e}\right) T_t \sqrt{\bar{C}_f}\, 7.50 - 11.24 M_e^2 \bar{C}_f T_t + 199 + 39.8 M_e^2\right]\left[\frac{T_w}{T_e} + 3.75\left(1 + 0.2M_e^2 - \frac{T_w}{T_e}\right)\sqrt{\bar{C}_f} - 3.75 M_e^2 \bar{C}_f\right]}{\left[\frac{T_w}{T_e} + 7.50\left(1 + 0.2M_e^2 - \frac{T_w}{T_e}\right)\sqrt{\bar{C}_f} - 11.24 M_e^2 \bar{C}_f\right]^{2.5}\left(T_t + 199 + 39.8 M_e^2\right)} \tag{A14}$$

Equations (A10) and (A14) are used to solve for $\bar{C}_f$, and C_f is then obtained from equation (A12).

Fenter-Stalmach Equations

The Fenter-Stalmach compressible law of the wall is given in reference 2 to be

$$\frac{U_e}{\sqrt{\frac{\tau_w}{\rho_w}}\sqrt{\sigma}} \sin^{-1}\left(\sqrt{\sigma}\,\frac{U}{U_e}\right) = f\left(\frac{y\rho_w}{\mu_w}\sqrt{\frac{\tau_w}{\rho_w}}\right) \tag{A15}$$

where

$$\sigma = \frac{\frac{\gamma - 1}{2} M_e^2}{1 + \frac{\gamma - 1}{2} M_e^2} \tag{A16}$$

and f is the functional expression of Coles incompressible law of the wall. In the fully turbulent region, this function is given analytically by

$$f\left(\frac{y\rho_w}{\mu_w}\sqrt{\frac{\tau_w}{\rho_w}}\right) = 5.75 \log_{10}\left(\frac{y\rho_w}{\mu_w}\sqrt{\frac{\tau_w}{\rho_w}}\right) + 5.1 \tag{A17}$$

Inserting equations (A16) and (A17) into equation (A15) and assuming $\gamma = 1.4$ results in

$$\frac{U_e}{\sqrt{\frac{\tau_w}{\rho_w}}} \frac{\sqrt{5 + M_e^2}}{M_e} \sin^{-1}\left(\frac{M}{\sqrt{5 + M_e^2}}\,\frac{U}{U_e}\right) = 5.75 \log_{10} \frac{y\rho_w}{\mu_w}\sqrt{\frac{\tau_w}{\rho_w}} + 5.1 \tag{A18}$$

but

$$\sqrt{\frac{\tau_w}{\rho_w}} \equiv \sqrt{\frac{C_f}{2}}\, U_e \sqrt{\frac{\rho_e}{\rho_w}}$$

and

$$\frac{y\rho_w}{\mu_w}\sqrt{\frac{\tau_w}{\rho_w}} \equiv R_y \sqrt{\frac{C_f}{2}}\,\frac{\mu_e}{\mu_w}\sqrt{\frac{\rho_w}{\rho_e}}$$

Thus equation (A18) becomes

$$\frac{\sqrt{2}}{\sqrt{C_f}}\sqrt{\frac{\rho_w}{\rho_e}}\,\frac{\sqrt{5+M_e^2}}{M_e}\,\sin^{-1}\left(\frac{M_e}{\sqrt{5+M_e^2}}\,\frac{U}{U_e}\right)=5.75\,\log_{10}\left(\frac{R_y\sqrt{C_f}}{\sqrt{2}}\,\frac{\mu_e}{\mu_w}\sqrt{\frac{\rho_w}{\rho_e}}\right)+5.1 \tag{A19}$$

Fenter and Stalmach make use of the viscosity power law of the form

$$\frac{\mu_e}{\mu_w}=\left(\frac{T_e}{T_w}\right)^{\omega} \tag{A20}$$

where ω is assumed to be 0.768 for air. Inserting equation (A20) into equation (A19) and assuming constant static pressure across the boundary layer results in

$$\frac{1}{\sqrt{C_f}}\sqrt{\frac{T_e}{T_w}}\,\frac{\sqrt{5+M_e^2}}{M_e}\,\sin^{-1}\left(\frac{M_e}{\sqrt{5+M_e^2}}\,\frac{U}{U_e}\right)=4.07\,\log_{10}\left[\frac{R_y\sqrt{C_f}}{\sqrt{2}}\left(\frac{T_e}{T_w}\right)^{1.268}\right]+3.61 \tag{A21}$$

or, finally

$$\frac{\sqrt{5+M_e^2}}{M_e\sqrt{\frac{T_w}{T_e}}}\,\sin^{-1}\left(\frac{M_e}{\sqrt{5+M_e^2}}\,\frac{U}{U_e}\right)=\sqrt{C_f}\left\{2.03\,\log_{10}\left[\frac{R_y^2C_f}{\left(\frac{T_w}{T_e}\right)^{2.536}}\right]+2.99\right\} \tag{A22}$$

Hopkins-Keener Equations

Hopkins and Keener (ref. 5) give the following equation for the fully turbulent part of their Preston tube calibration

$$\log_{10}\left[f_2(T')R_d^2\left(\frac{M}{M_e}\right)^2\right]=1.132\,\log_{10}\left[f_2(T')R_d^2C_f\right]+1.517 \tag{A23}$$

where

$$f_2(T')=\left(\frac{\mu_e}{\mu'}\right)^2\frac{\rho'}{\rho_e} \tag{A24}$$

Assuming constant static pressure through the boundary layer and Sutherland's viscosity law results in

$$f_2(T')=\left(\frac{T_e}{T'}\right)^4\left(\frac{T'+199}{T_e+199}\right)^2 \tag{A25}$$

Hopkins and Keener use Sommer and Short's T' equation $\left(T'/T_e=0.55+0.035\,M_e^2+0.45\,T_w/T_e\right)$ so that equation (A25) may be written as

$$f_2(T')=\frac{\left(0.55\,T_t+0.035T_tM_e^2+0.45T_t\,\frac{T_w}{T_e}+199+39.8\,M_e^2\right)^2}{\left(0.55+0.035M_e^2+0.45\,\frac{T_w}{T_e}\right)^4\left(T_t+199+39.8M_e^2\right)^2} \tag{A26}$$

Inserting equation (A26) into equation (A23) yields

$$C_f = \frac{\left(\frac{M}{M_e}\right)^{1.767}\left(0.55 + 0.035M_e^2 + 0.45\frac{T_w}{T_e}\right)^{0.466}\left(T_t + 199 + 39.8M_e^2\right)^{0.233}}{21.9R_d^{0.233}\left(0.55T_t + 0.035T_tM_e^2 + 0.45T_t\frac{T_w}{T_e} + 199 + 39.8M_e^2\right)^{0.233}} \tag{A27}$$

In this study R_d is replaced by $2R_y$ so that the calibration may be used to calculate skin friction from conventional velocity profiles. Also, constant total temperature is assumed across the boundary layer so that

$$\frac{M}{M_e} = \frac{U/U_e}{\sqrt{1 + 0.2M_e^2\left[1 - \left(\frac{U}{U_e}\right)^2\right]}} \tag{A28}$$

Making these substitutions into equation (A27) yields the final Hopkins-Keener equation

$$C_f = \frac{\left(\frac{U}{U_e}\right)^{1.767}\left(0.55 + 0.035M_e^2 + 0.45\frac{T_w}{T_e}\right)^{0.466}\left(T_t + 199 + 39.8M_e^2\right)^{0.233}}{25.7\left\{1 + 0.2\,M_e^2\left[1 - \left(\frac{U}{U_e}\right)^2\right]\right\}^{0.884} R_y^{0.233}\left(0.55\,T_t + 0.035T_tM_e^2 + 0.45T_t\frac{T_w}{T_e} + 199 + 39.8\,M_e^2\right)^{0.233}} \tag{A29}$$

Sigalla Equations

Reference 6 gives the Sigalla Preston tube calibration to be

$$\frac{\rho' d^2\tau_w}{\mu'^2} = 0.0529\left(\frac{\rho' d^2\Delta p}{\mu'^2}\right)^{0.873} \tag{A30}$$

where Δp is given to be

$$\Delta p = \frac{1}{2}\rho' U^2 \tag{A31}$$

Hence,

$$\frac{\rho' d^2\tau_w}{\mu'^2} = 0.0529\left(\frac{\rho'^2 d^2 U^2}{2\mu'^2}\right)^{0.873}$$

APPENDIX

Assuming constant static pressure across the boundary layer, Sutherland's viscosity law, Sommer and Short's reference temperature, and $d = 2y$ results in

$$C_f = \frac{0.04844\left(\frac{U}{U_e}\right)^{1.746}\left(T_t + 199 + 39.8M_e^2\right)^{0.254}}{R_y^{0.254}\left(0.55 + 0.035M_e^2 + 0.45\frac{T_w}{T_e}\right)^{0.365}\left(0.55T_t + 0.035T_tM_e^2 + 0.45\frac{T_w}{T_e}T_t + 199 + 39.8M_e^2\right)^{0.254}} \quad \text{(A32)}$$

REFERENCES

1. Clauser, Francis H.: Turbulent Boundary Layers in Adverse Pressure Gradients. J. Aeronaut. Sci., vol. 21, no. 2, Feb. 1954, pp. 91-108.

2. Fenter, Felix W.; and Stalmach, Charles J., Jr.: The Measurement of Local Turbulent Skin Friction at Supersonic Speeds by Means of Surface Impact Pressure Probes. DRL 392, CM 878 (Contract NOrd-16498), Univ. of Texas, Oct. 21, 1957.

3. Baronti, Paolo O.; and Libby, Paul A.: Velocity Profiles in Turbulent Compressible Boundary Layers. AIAA J., vol. 4, no. 2, Feb. 1966, pp. 193-202.

4. Coles, D. E.: The Turbulent Boundary Layer in a Compressible Fluid. U.S. Air Force Proj. RAND Rept. R-403-PR, The RAND Corp., Sept. 1962.

5. Hopkins, Edward J.; and Keener, Earl R.: Study of Surface Pitots for Measuring Turbulent Skin Friction at Supersonic Mach Numbers – Adiabatic Wall. NASA TN D-3478, 1966.

6. Sigalla, Armand: Calibration of Preston Tubes in Supersonic Flow. AIAA J. (Tech. Notes), vol. 3, no. 8, Aug. 1965, p. 1531.

7. Jackson, Mary W.; Czarnecki, K. R.; and Monta, William J.: Turbulent Skin Friction at High Reynolds Numbers and Low Supersonic Velocities. NASA TN D-2687, 1965.

8. Lobb, R. Kenneth; Winkler, Eva M.; and Persh, Jerome: Experimental Investigation of Turbulent Boundary Layers in Hypersonic Flow. J. Aeronaut. Sci., vol. 22, no. 1, Jan. 1955, pp. 1-9.

9. Winkler, Eva M.; and Cha, Moon H.: Investigation of Flat Plate Hypersonic Turbulent Boundary Layers With Heat Transfer at a Mach Number of 5.2. NAVORD Rep. 6631, U.S. Naval Ord. Lab., Sept. 15, 1959.

10. Coles, Donald: Measurements in the Boundary Layer on a Smooth Flat Plate in Supersonic Flow III. Measurements in a Flat-Plate Boundary Layer at the Jet Propulsion Laboratory. Rept. No. 20-71 (Contract No. DA-04-495-Ord 18), Jet Propulsion Lab., California Inst. Technol., June 1, 1953.

11. Matting, Fred W.; Chapman, Dean R.; Nyholm, Jack R.; and Thomas, Andrew G.: Turbulent Skin Friction at High Mach Numbers and Reynolds Numbers in Air and Helium. NASA TR R-82, 1961.

12. Moore, D. R.; and Harkness, J.: Experimental Investigation of the Compressible Turbulent Boundary Layer at Very High Reynolds Numbers. AIAA J., vol. 3, no. 4, Apr. 1965, pp. 631-638.

13. Shutts, W. H.; Hartwig, W. H.; and Weiler, J. E.: Final Report on Turbulent Boundary-Layer and Skin-Friction Measurements on a Smooth, Thermally Insulated Flat Plate at Supersonic Speeds. DRL-364, CM-823 (Contract NOrd-9195), Univ. of Texas, Jan. 5, 1955.

14. Stalmach, Charles J., Jr.: Experimental Investigation of the Surface Impact Pressure Probe Method of Measuring Local Skin Friction at Supersonic Speeds. DRL-410, CF-2675 (Contract NOrd-16498), Univ. of Texas, Jan. 1958.

15. Bertram, Mitchel H.; Cary, Aubrey M., Jr.; and Whitehead, Allen H., Jr.: Experiments with Hypersonic Turbulent Boundary Layers on Flat Plates and Delta Wings. Paper presented at AGARD Specialists' Meeting on Hypersonic Boundary Layers and Flow Fields. (London, England), May 1-3, 1968.

16. Spalding, D. B.; and Chi, S. W.: The Drag of a Compressible Turbulent Boundary Layer on a Smooth Flat Plate With and Without Heat Transfer. J. Fluid Mech., vol. 18, pt. 1, Jan. 1964, pp. 117-143.

TABLE I.- SUMMARY OF RESULTS

Profile	M_e	R/cm	T_t, °K	T_w/T_{aw}	Skin friction calculated from method of –				Experimental C_f (balance)	R_θ
					Hopkins-Keener	Fenter-Stalmach	Baronti-Libby	Sigalla		
					Hopkins-Keener (unpublished)					
1	2.445	0.0824×10^6	314	1	0.001428	0.001336	0.001255	0.001155	0.001260	59 680
2	2.961	.0806	325	1	.001254	.001221	.001107	.001049	.001110	55 590
3	3.443	.0787	328	1	.001212	.001072	.000964	.000946	.000910	53 740
4	2.468	.1073	323	1	.001366	.001280	.001198	.001063	.001270	75 260
5	2.978	.1036	339	1	.001272	.001198	.001070	.000988	.001100	68 140
					Jackson et al. (ref. 7)					
6	1.604	0.2661×10^6	316	1	0.001554	0.001613	0.001581	0.001798	0.001620	80 156
7	1.592	.0279	316	1	.002026	.002113	.002196	.002197	.002170	10 845
8	2.182	.2098	316	1	.001500	.001441	.001381	.001279	.001444	50 989
9	2.179	.1774	316	1	.001536	.001473	.001421	.001338	.001461	43 716
10	2.188	.1453	316	1	.001572	.001505	.001459	.001384	.001485	36 860
11	2.187	.1089	316	1	.001622	.001559	.001521	.001467	.001530	29 198
12	2.182	.0724	316	1	.001667	.001622	.001612	.001585	.001614	20 974
13	2.185	.0367	316	1	.001822	.001814	.001817	.001831	.001766	11 132
14	2.146	.0216	316	1	.001890	.001917	.001961	.001987	.001865	7 556
15	1.595	.2659	316	1	.001545	.001603	.001579	.001667	.001620	83 872
16	1.595	.2256	316	1	.001598	.001644	.001620	.001758	.001660	72 030
17	1.590	.1372	316	1	.001775	.001787	.001768	.001880	.001760	45 061
18	1.591	.0924	316	1	.001914	.001900	.001893	.002031	.001860	30 511
19	1.588	.0462	316	1	.002030	.002049	.002088	.002144	.002080	17 090
20	1.593	.1829	316	1	.001665	.001699	.001676	.001759	.001700	58 977
21	2.115	.0222	316	1	.001774	.001794	.001830	.001856	.001654	9 657
22	2.172	.0370	316	1	.001717	.001710	.001707	.001720	.001636	13 799
23	2.178	.0730	316	1	.001632	.001573	.001545	.001507	.001505	25 216
24	2.192	.1096	316	1	.001556	.001487	.001450	.001385	.001449	35 099
25	2.198	.1443	316	1	.001511	.001445	.001398	.001312	.001400	44 303
26	2.200	.1764	316	1	.001476	.001419	.001358	.001257	.001404	52 405
27	2.202	.2075	316	1	.001439	.001386	.001332	.001214	.001387	60 112
28	2.172	.0367	316	1	.001663	.001669	.001664	.001691	.001636	14 510
29	2.159	.1083	316	1	.001463	.001453	.001437	.001384	.001449	35 508
30	2.188	.1441	316	1	.001493	.001447	.001404	.001319	.001400	44 672
31	2.192	.1789	316	1	.001461	.001408	.001365	.001261	.001404	52 248
32	2.192	.2091	316	1	.001430	.001385	.001335	.001218	.001387	59 844
33	2.163	.0735	316	1	.001576	.001554	.001532	.001496	.001505	26 336
34	2.161	.0367	316	1	.001836	.001776	.001754	.001750	.001636	13 586
35	2.110	.0222	316	1	.001616	.001714	.001772	.001809	.001654	9 723
36	2.186	.0722	316	1	.001415	.001403	.001387	.001336	.001365	37 982
37	2.194	.2085	316	1	.001317	.001289	.001236	.001105	.001256	94 481
38	2.188	.1443	316	1	.001380	.001341	.001293	.001226	.001289	63 929
39	2.195	.2093	316	1	.001334	.001303	.001240	.001106	.001256	85 542
40	2.192	.1770	316	1	.001368	.001331	.001274	.001152	.001286	73 696
41	2.189	.1443	316	1	.001408	.001363	.001317	.001203	.001289	61 403
42	2.182	.1081	316	1	.001456	.001406	.001361	.001272	.001324	49 008
43	2.142	.0365	316	1	.001606	.001552	.001547	.001542	.001484	21 061
44	2.083	.0220	316	1	.001627	.001640	.001644	.001679	.001544	13 360
45	2.172	.1772	316	1	.001398	.001361	.001320	.001215	.001369	60 685

TABLE I.- SUMMARY OF RESULTS – Continued

Profile	M_e	R/cm	T_t, °K	T_w/T_{aw}	Skin friction calculated from method of –				Experimental C_f (balance)	R_θ
					Hopkins-Keener	Fenter-Stalmach	Baronti-Libby	Sigalla		
Jackson et al. (ref. 7)										
46	2.165	0.1085×10^6	316	1	0.001491	0.001446	0.001410	0.001343	0.001454	40 131
47	2.138	.0366	316	1	.001575	.001581	.001604	.001614	.001690	17 131
48	2.170	.1780	316	1	.001365	.001332	.001286	.001176	.001271	68 974
49	2.169	.1085	316	1	.001461	.001418	.001381	.001301	.001324	45 284
50	2.115	.0365	316	1	.001575	.001562	.001558	.001550	.001522	19 159
51	2.199	.1443	316	1	.001371	.001333	.001286	.001179	.001289	65 500
52	2.149	.0364	316	1	.001504	.001522	.001539	.001535	.001484	21 008
53	1.587	.2650	316	1	.001353	.001442	.001425	.001167	.001408	123 836
54	1.594	.2256	316	1	.001387	.001472	.001451	.001192	.001430	107 318
55	1.594	.1835	316	1	.001442	.001506	.001493	.001237	.001463	91 405
56	1.587	.1373	316	1	.001510	.001562	.001552	.001317	.001520	72 236
57	1.575	.0915	316	1	.001629	.001655	.001657	.001443	.001623	50 908
58	1.548	.0460	316	1	.001736	.001818	.001856	.001722	.001821	26 317
59	1.469	.0273	316	1	.001786	.001852	.001945	.001930	.001993	15 675
60	1.599	.2219	316	1	.001524	.001582	.001559	.001298	.001550	78 918
61	1.602	.2699	316	1	.001468	.001536	.001515	.001650	.001530	93 874
62	1.598	.1823	316	1	.001574	.001621	.001600	.001832	.001580	67 789
63	1.593	.1370	316	1	.001653	.001680	.001667	.001921	.001650	52 482
64	1.586	.0918	316	1	.001780	.001784	.001787	.002053	.001770	35 864
65	1.567	.0466	316	1	.001937	.001990	.002021	.002132	.001950	18 258
66	1.555	.0277	316	1	.002066	.002079	.002129	.002101	.002080	11 703
67	1.598	.2256	316	1	.001462	.001530	.001510	.001573	.001530	89 760
68	1.597	.1372	316	1	.001581	.001620	.001607	.001702	.001616	60 359
69	1.579	.0462	316	1	.001890	.001932	.001953	.002038	.001934	20 816
70	1.596	.2262	316	1	.001411	.001484	.001468	.001564	.001540	101 828
71	1.596	.1376	316	1	.001533	.001582	.001568	.001733	.001590	67 108
72	1.579	.0462	316	1	.001907	.001908	.001921	.001746	.001860	23 077
Coles (ref. 10)										
73	1.966	0.0315×10^6	306	1	0.002371	0.002398	0.002490	0.002487	0.002720	2 980
74	1.978	.0794	302	1	.001922	.001965	.002046	.002074	.002180	6 470
75	1.982	.1133	303	1	.001876	.001864	.001928	.001970	.002020	8 570
76	2.540	.0308	306	1	.002549	.002425	.002487	.002500	.002420	2 190
77	2.568	.0887	309	1	.001795	.001739	.001785	.001835	.001810	6 600
78	2.578	.1525	316	1	.001559	.001579	.001585	.001633	.001660	10 200
79	3.690	.0380	306	1	.002330	.001977	.001981	.002036	.002110	2 120
80	3.701	.0649	312	1	.001637	.001499	.001555	.001607	.001620	4 100
81	3.697	.1329	312	1	.001363	.001268	.001302	.001372	.001380	7 560
82	4.512	.0645	306	1	.001643	.001359	.001432	.001464	.001480	3 470
83	4.554	.1252	308	1	.001301	.001120	.001171	.001230	.001220	6 590
84	4.545	.1267	312	1	.001583	.001253	.001329	.001371	.001310	4 980
85	4.504	.1282	314	1	-------	.001556	.001655	.001597	.001550	2 900
86	4.544	.1274	313	1	.001553	.001236	.001255	.001332	.001260	5 240

TABLE I.- SUMMARY OF RESULTS – Continued

Profile	M_e	R/cm	T_t, °K	T_w/T_{aw}	Skin friction calculated from method of –				Experimental C_f (balance)	R_θ
					Hopkins-Keener	Fenter-Stalmach	Baronti-Libby	Sigalla		
					Matting et al. (ref. 11)					
87	2.95	0.1587×10^6	333	1	0.001990	0.001679	0.001607	0.001682	0.001540	8 050
88	2.95	.4992	333	1	.001705	.001427	.001309	.001328	.001290	21 570
89	4.20	.1425	333	1	.001954	.001299	.001287	.001405	.001270	6 150
90	4.20	.6398	333	1	.001190	.000981	.000931	.001004	.000952	22 750
91	4.20	1.1382	333	1	.001152	.000967	.000832	.000893	.000868	37 580
					Moore and Harkness (ref. 12)					
92	2.669	0.8650×10^6	304	1	0.000829	0.000845	0.000787	0.000862	0.000862	702 000
					Shutts et al. (ref. 13)					
93	1.724	0.2205×10^6	339	1	0.002265	0.002285	0.002326	0.002309	0.002225	6 082
94	1.724	.2205	339	1	.002303	.002279	.002300	.002289	.002225	6 093
95	1.782	.2222	339	1	.001932	.001922	.001943	.001908	.001947	11 644
96	1.726	.2228	339	1	.001899	.001866	.001839	.001749	.001784	19 833
97	2.017	.2469	339	1	.002336	.002181	.002149	.002143	.002060	6 113
98	1.996	.2478	339	1	.002041	.001962	.001932	.001921	.001810	11 015
99	2.000	.2458	339	1	.001797	.001744	.001720	.001658	.001635	20 090
100	2.249	.2422	339	1	.002000	.001940	.001993	.002031	.001985	6 182
101	2.242	.2401	339	1	.002038	.001917	.001909	.001937	.001816	8 301
102	2.236	.2396	339	1	.001908	.001837	.001801	.001817	.001704	10 711
103	2.243	.2387	339	1	.001748	.001631	.001583	.001562	.001623	20 490
104	2.502	.2455	339	1	.002096	.001937	.001939	.001991	.001804	6 085
105	2.533	.2455	339	1	.001963	.001784	.001724	.001768	.001583	9 639
106	2.451	.2455	339	1	.001734	.001618	.001548	.001529	.001560	18 811
					Stalmach (ref. 14)					
107	1.739	0.3854×10^6	303	1	0.001901	0.001880	0.001916	0.001906	0.001955	12 490
108	1.744	.3827	303	1	.001893	.001884	.001930	.001919	.001995	12 240
109	1.744	.2460	298	1	.002039	.002048	.002102	.002095	.002117	8 429
110	1.739	.1418	298	1	.002491	.002512	.002592	.002604	.002610	3 589
111	1.737	.1391	299	1	.002581	.002593	.002697	.002677	.002559	3 443
112	2.019	.4093	303	1	.001913	.001857	.001881	.001855	.001885	12 320
113	2.009	.2176	299	1	.002044	.002018	.002072	.002078	.002095	7 528
114	2.007	.1281	298	1	.002609	.002585	.002685	.002680	.002603	2 899
115	2.238	.4037	306	1	.001797	.001737	.001770	.001776	.001767	11 670
116	2.227	.2180	299	1	.001955	.001926	.001985	.002012	.001994	6 892
117	2.230	.1145	301	1	.002745	.002636	.002678	.002694	.002575	2 520
118	2.490	.4080	308	1	.001712	.001672	.001663	.001693	.001651	11 400
119	2.483	.2084	303	1	.001925	.001907	.001931	.001978	.001872	6 097
120	2.502	.2066	300	1	.001889	.001870	.001923	.001967	.001872	6 072
121	2.484	.1047	302	1	.002673	.002409	.002452	.002477	.002494	2 660
122	2.739	.4374	304	1	.001754	.001577	.001549	.001597	.001492	11 900
123	2.724	.2179	303	1	.002057	.001840	.001830	.001888	.001802	6 304
124	2.729	.1140	295	1	.002295	.002194	.002224	.002273	.002215	3 048
125	2.949	.4218	305	1	.001614	.001516	.001488	.001545	.001495	11 400
126	2.949	.2156	299	1	.001895	.001767	.001759	.001824	.001708	6 041
127	2.958	.1093	295	1	.002346	.002219	.002187	.002252	.002160	2 740

TABLE I.- SUMMARY OF RESULTS – Concluded

Profile	M_e	R/cm	T_t, °K	T_w/T_{aw}	Skin friction calculated from method of – Hopkins-Keener	Fenter-Stalmach	Baronti-Libby	Sigalla	Experimental C_f (balance)	R_θ
				Stalmach (ref. 14)						
128	3.161	0.4294×10^6	306	1	0.001623	0.001423	0.001401	0.001468	0.001407	11 310
129	3.168	.2561	294	1	.001787	.001573	.001585	.001641	.001594	7 149
130	3.166	.1068	304	1	.002437	.002119	.002097	.002180	.001997/0.002144	2 651
131	3.389	.4337	303	1	.001547	.001350	.001328	.001403	.001325	11 270
132	3.402	.2737	297	1	.001531	.001407	.001414	.001487	.001452	7 785
133	3.400	.1118	298	1	.002267	.001992	.001981	.002060	.002016	2 758
134	3.681	.3906	303	1	.001359	.001224	.001233	.001312	.001243	10 180
135	3.681	.3948	303	1	.001335	.001230	.001247	.001326	.001243	9 836
136	3.667	.2814	297	1	.001341	.001290	.001325	.001401	.001293	7 991
137	3.672	.0894	299	1	.002577	.002116	.002016	.002097	.002057	2 096
138	3.684	.0897	298	1	.002501	.002085	.001981	.002116	.002057	2 075

Profile	M_e	R/cm	T_t, °K	T_w/T_{aw}	Skin friction calculated from method of – Hopkins-Keener	Fenter-Stalmach	Baronti-Libby	Sigalla	Experimental C_f (velocity slope/ heat transfer)	R_θ
				Lobb et al. (ref. 8)						
139	4.93	0.0857×10^6	326	1.03	0.001421	0.001177	0.001196	0.001276	0.001090	5 350
140	5.01	.0915	399	.79	.001148	.001232	.001361	.001302	.001090/0.001060	6 480
141	5.03	.0976	513	.64	.001024	.001285	.001323	.001267	.000943/0.000969	7 950
142	5.06	.0846	562	.59	.001034	.001386	.001390	.001332	.000918	7 370
143	5.75	.1804	401	.91	.000842	.000792	.000836	.000888	.000820/0.000800	11 600
144	5.79	.1665	477	.78	.000849	.000897	.000874	.000939	.000725/0.000719	12 400
145	5.82	.1318	550	.63	.000779	.001009	.000943	.001022	.000710/0.000692	11 400
146	6.83	.1091	467	.69	.000399	.000615	.000760	.000965	.000683/0.000666	8 550
147	6.78	.1018	586	.57	.000910	.000923	.000872	.000928	.000666/0.000665	8 400
148	6.83	.1400	586	.57	.000597	.000826	.000797	.000845	.000593/0.000582	12 640
149	6.78	.0902	639	.51	.000658	.001105	.000944	.000994	.000694/0.000670	7 960
150	7.67	.0773	645	.52	.000438	.000820	.000809	.000860	.000598	8 130
151	8.18	.0837	655	.52	.000472	.000824	.000810	.000821	.000530/0.000496	9 540
				Winkler et al. (ref. 9)						
152	5.21	0.1265×10^6	382	0.889	-------	0.001707	0.001857	0.001709	0.001465/0.001487	2 099
153	5.14	.1554	345	.976	0.002681	.001562	.001782	.001631	.001389	2 936
154	5.20	.1392	366	.933	-------	.001477	.001735	.001564	.001432/0.001348	3 173
155	5.26	.1366	364	.926	.001654	.001376	.001587	.001446	.001346/0.001343	3 880
156	5.29	.1335	362	.939	-------	.001222	.001208	.001301	.001308/0.001276	4 300
157	4.98	.1061	383	.841	-------	.001890	.001130	-------	.001335/0.001348	1 900
158	5.18	.1196	398	.826	-------	.001930	.002088	.001876	.001606	1 782
159	5.20	.1304	373	.835	-------	.001618	.001806	.001656	.001248/0.001165	2 960
160	5.24	.1234	379	.860	-------	.001441	.001297	.001431	.001151/0.001170	3 455
161	5.24	.1148	384	.852	-------	.001208	.001401	.001394	/0.001063	3 790
162	5.17	.0926	455	.682	-------	.001596	.001843	.001547	.001470/0.001547	1 055
163	5.16	.0879	476	.651	-------	.002236	.002272	.002058	.001323/0.001335	1 652
164	5.10	.0933	468	.642	.002616	.002211	.002314	.002125	.001335	1 735
165	5.20	.0970	466	.654	.002081	.001910	.001547	.001707	.001203	2 482
166	5.11	.0885	496	.627	.002128	.001997	.001547	.001726	.001236/0.001279	2 488
167	5.12	.0949	465	.670	.001890	.001746	.001407	.001575	.001054/0.001075	3 256

TABLE II.- C_f CALCULATED FROM BARONTI-LIBBY TRANSFORMATION

[Profile 26]

y, cm	U/U_e	$\overline{C}_f$	C_f	y, cm	U/U_e	$\overline{C}_f$	C_f
0.0114	0.5468	0.003360	0.002030	0.7277	0.8018	0.002350	0.001366
.0165	.5623	.003148	.001885	.8547	.8135	.002340	[a].001358
.0216	.5764	.003035	.001809	1.0071	.8297	.002345	.001363
.0266	.5870	.002943	.001752	1.1595	.8432	.002350	.001366
.0368	.6028	.002825	.001670	1.3500	.8592	.002363	.001373
.0455	.6163	.002795	.001649	1.5151	.8709	.002373	.001377
.0546	.6276	.002726	.001609	1.7056	.8860	.002388	.001390
.0673	.6405	.002685	.001578	1.8961	.8982	.002405	.001397
.0800	.6515	.002644	.001555	2.0866	.9128	.002428	.001414
.0927	.6604	.002617	.001535	2.2771	.9223	.002435	.001418
.1181	.6776	.002585	.001513	2.5311	.9376	.002458	.001433
.1434	.6912	.002556	.001496	2.7978	.9527	.002486	.001449
.1687	.7013	.002535	.001477	3.0518	.9649	.002495	.001460
.1943	.7114	.002506	.001466	3.3058	.9749	.002506	.001466
.2196	.7197	.002495	.001455	3.5598	.9836	.002516	.001470
2578	.7296	.002468	.001438	3.8138	.9885	.002506	.001465
.3085	.7410	.002440	.001421	4.1948	.9925	.002486	.001449
.3722	.7531	.002413	.001404	4.8298	.9969	.002440	.001422
.4483	.7649	.002394	.001387	5.5918	.9991	.002394	.001389
.5245	.7768	.002373	.001380	6.3538	1.0003	.002341	.001360
.6134	.7884	.002363	.001372	7.1158	1.0000	.002295	.001332

[a]Value of C_f chosen for profile.

TABLE III.- C_f CALCULATED FROM THE PRESTON TUBE CALIBRATION OF FENTER-STALMACH, HOPKINS-KEENER, AND SIGALLA

[Profile 26]

y, cm	U/U_e	M/M_e	Fenter-Stalmach	Hopkins-Keener	Sigalla
0.0114	0.5468	0.4220	0.001879	0.001637	0.001936
.0165	.5623	.4362	.001766	.001592	.001852
.0216	.5764	.4492	.001707	.001576	.001806
.0266	.5870	.4591	.001663	.001559	.001767
.0368	.6028	.4742	.001599	.001530	.001705
.0455	.6163	.4872	.001585	.001537	.001690
.0546	.6276	.4982	.001555	.001524	.001655
.0673	.6405	.5110	.001533	.001518	.001626
.0800	.6515	.5221	.001518	.001514	.001604
.0927	.6604	.5312	.001503	.001508	.001582
.1181	.6776	.5490	.001492	.001511	.001556
.1434	.6912	.5633	.001482	.001511	.001533
.1687	.7013	.5742	.001470	.001504	.001508
.1943	.7114	.5851	.001465	.001506	.001492
.2196	.7197	.5943	.001459	.001504	.001476
.2578	.7296	.6053	.001448	.001497	.001452
.3085	.7410	.6183	.001438	.001490	.001425
.3722	.7531	.6322	.001429	.001483	.001398
.4483	.7649	.6461	.001419	[a].001476	.001370
.5245	.7768	.6603	.001419	.001479	.001352
.6134	.7884	.6745	.001418	.001480	.001334
.7277	.8018	.6912	.001420	.001485	.001315
.8547	.8135	.7061	[a].001419	.001485	.001295
1.0071	.8297	.7272	.001434	.001506	.001285
1.1595	.8432	.7454	.001445	.001522	.001276
1.3500	.8592	.7674	.001462	.001547	.001268
1.5151	.8709	.7841	.001474	.001564	.001261
1.7056	.8860	.8061	.001497	.001598	.001261
1.8961	.8982	.8244	.001514	.001622	[a].001257
2.0866	.9128	.8470	.001542	.001664	.001262
2.2771	.9223	.8621	.001554	.001682	.001257
2.5311	.9376	.8871	.001582	.001726	.001259
2.7978	.9527	.9128	.001612	.001773	.001262
3.0518	.9649	.9342	.001635	.001811	.001262
3.3058	.9749	.9523	.001651	.001838	.001260
3.5598	.9836	.9685	.001665	.001861	.001255
3.8138	.9885	.9777	.001665	.001863	.001244
4.1948	.9925	.9854	.001654	.001847	.001223
4.8298	.9969	.9939	.001633	.001815	.001189
5.5918	.9991	.9982	.001604	.001767	.001150
6.3538	1.0003	1.0006	.001576	.001723	.001116
7.1158	1.0000	1.0000	.001547	.001676	.001084

[a]Value of C_f chosen for profile.

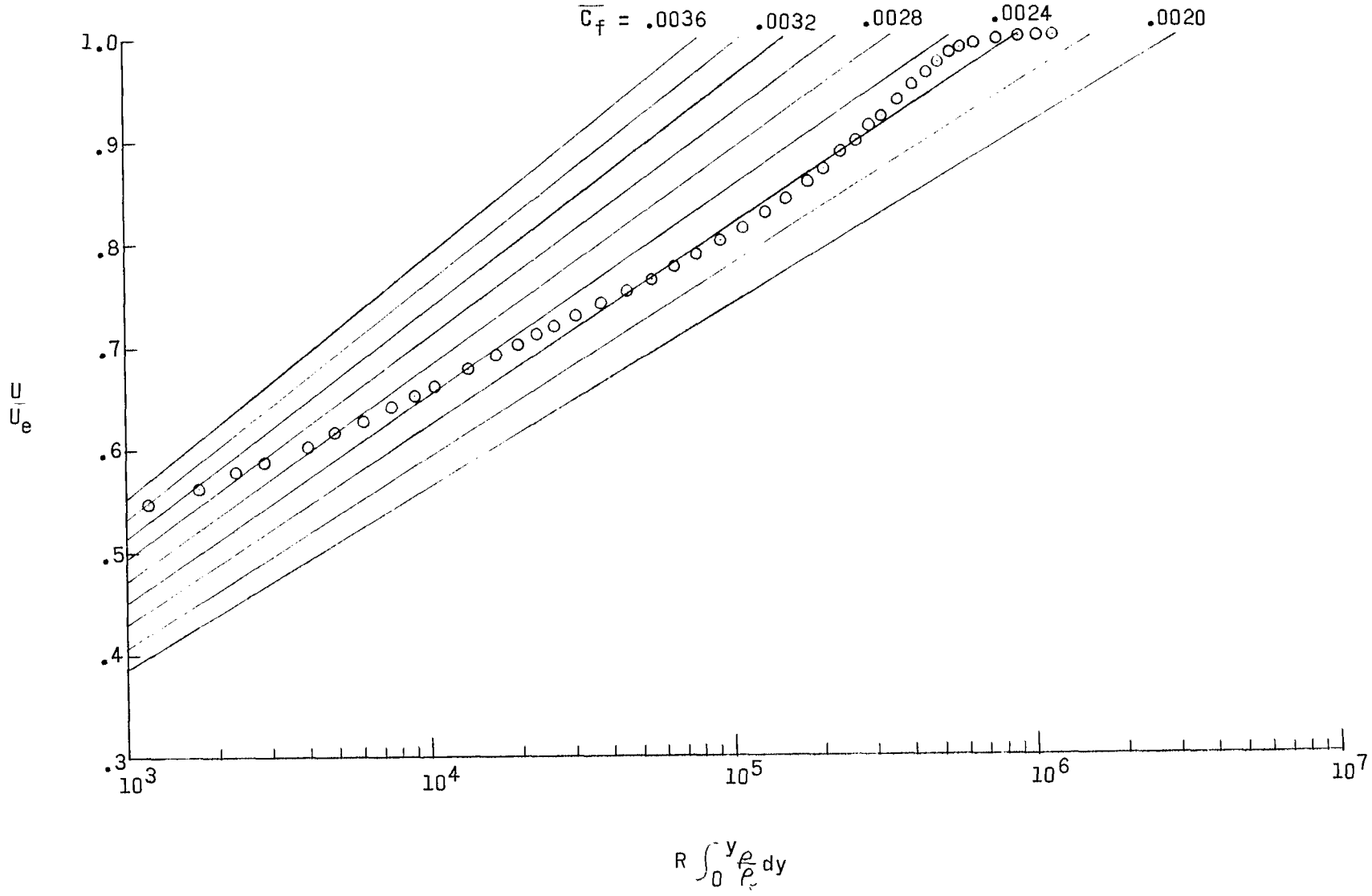

Figure 1.- Sample plot illustrating Baronti-Libby technique. Profile 26; M_e = 2.2; R = 0.176 × 10^6/cm; T_t = 316° K.

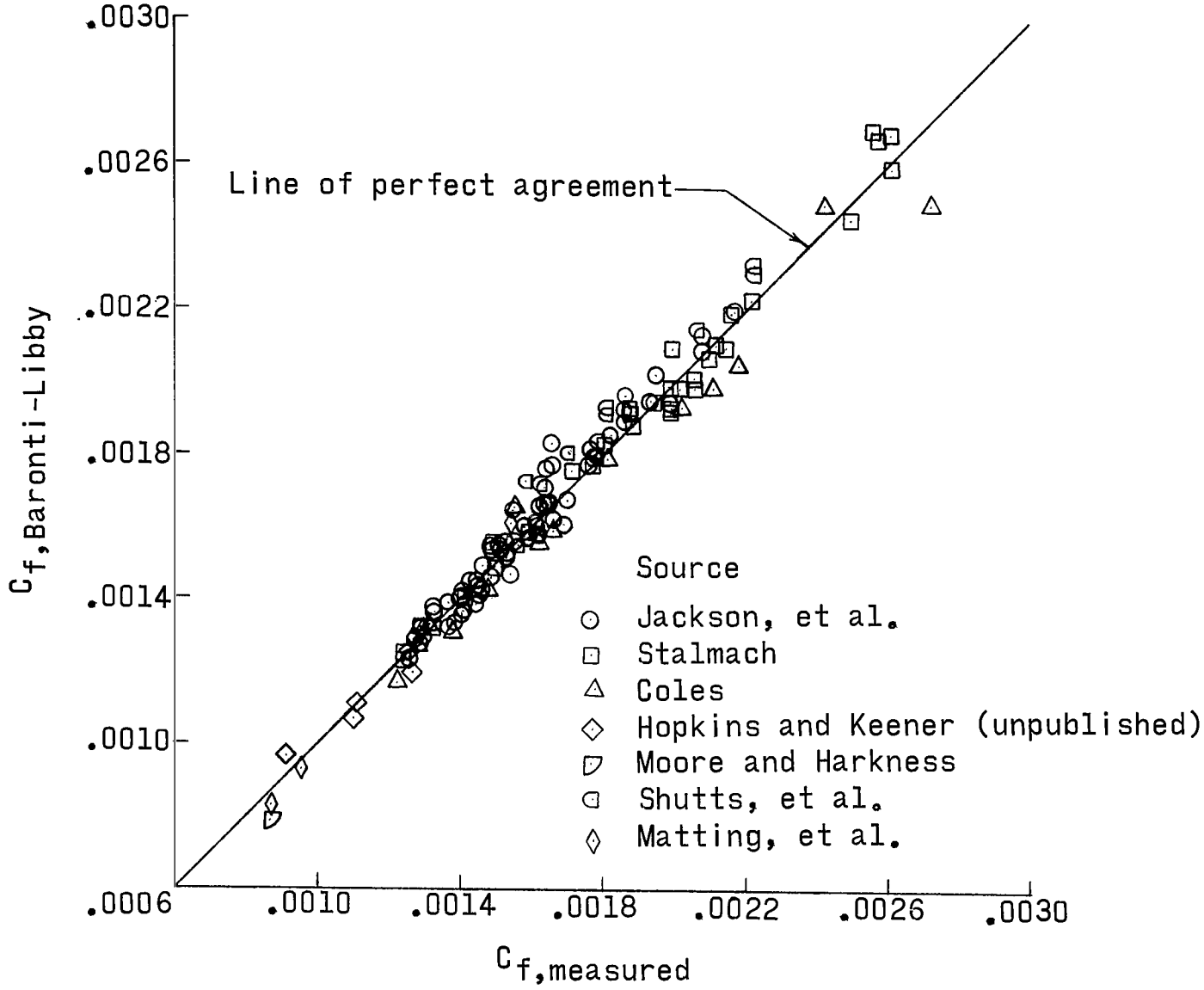

Figure 2.- Comparison between calculated and measured skin friction – Baronti-Libby method.

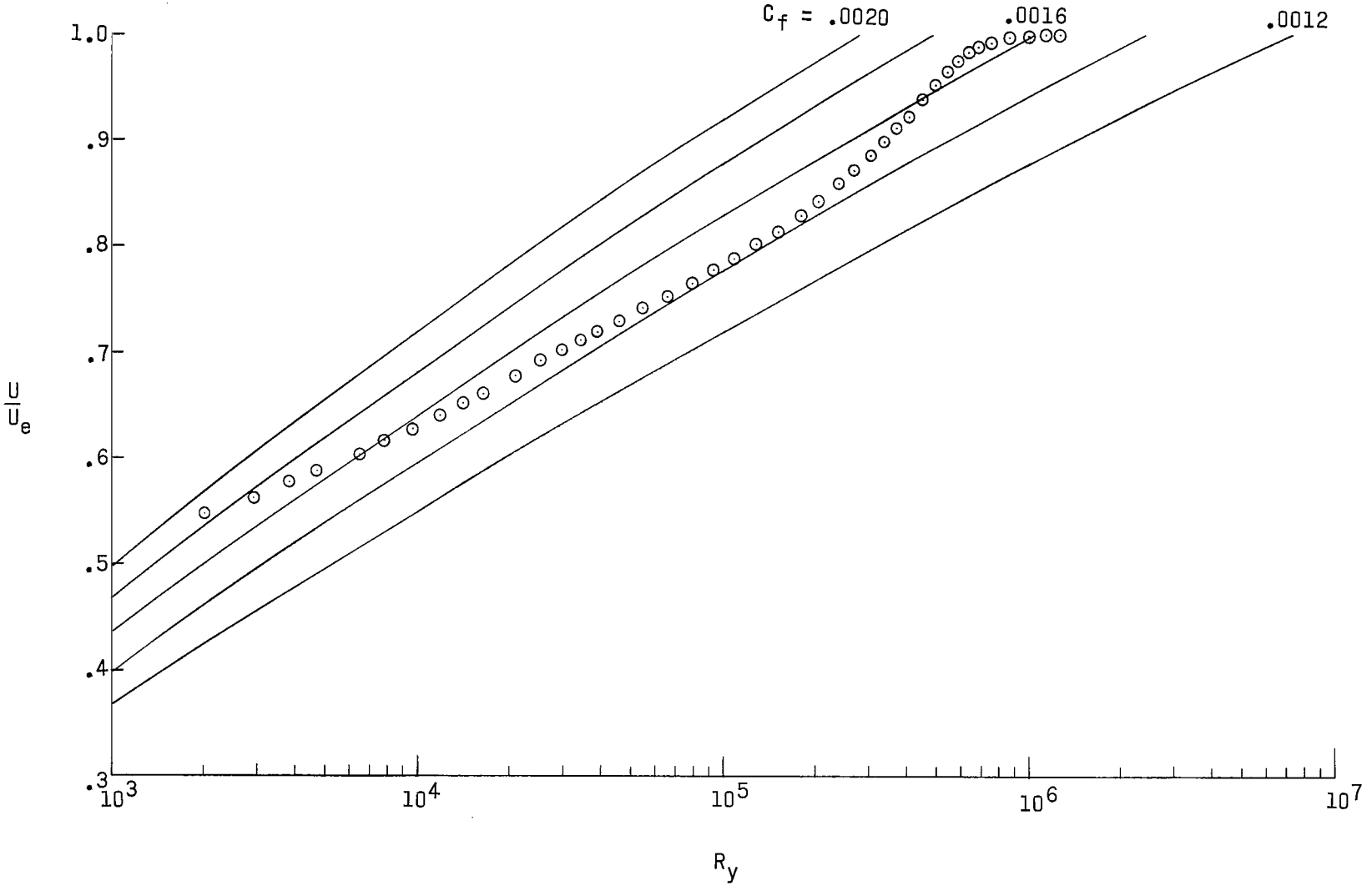

(a) Fenter-Stalmach.

Figure 3.- Sample profile compared with Preston tube calibration. Profile 26; $M_e = 2.2$; $R = 0.176 \times 10^6/cm$; $T_t = 316^0$ K.

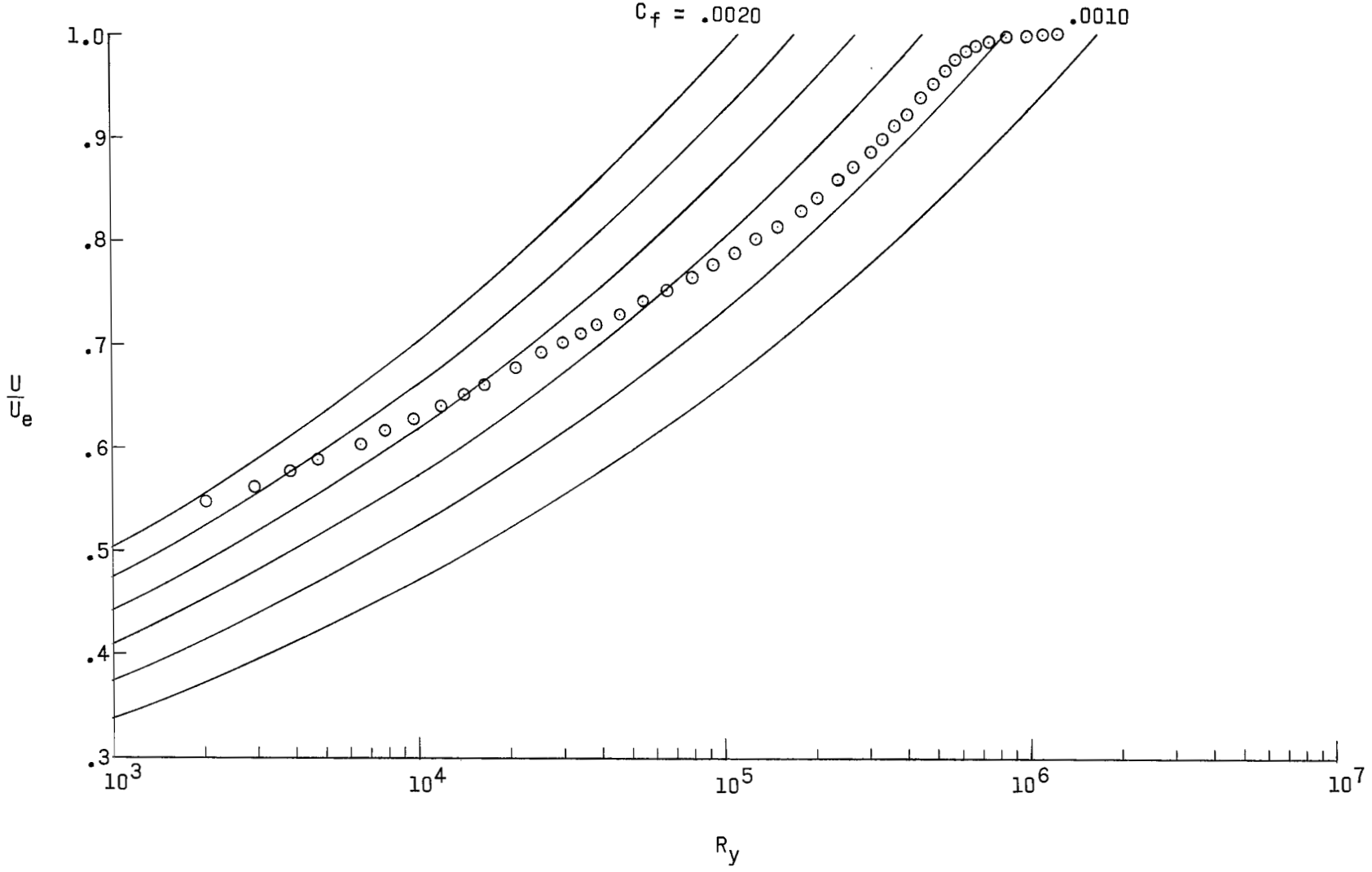

(b) Sigalla.

Figure 3.- Continued.

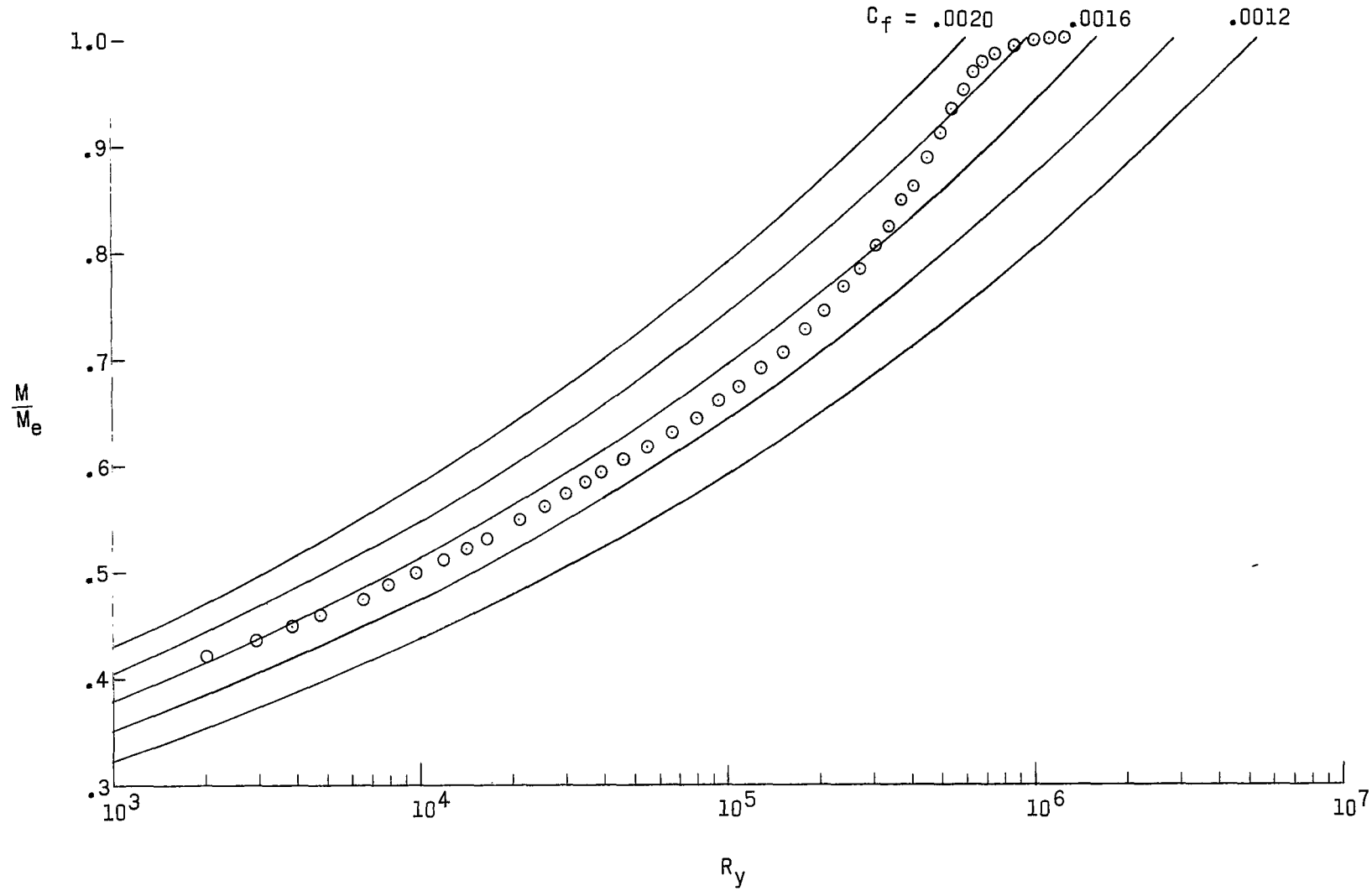

(c) Hopkins-Keener.

Figure 3.- Concluded.

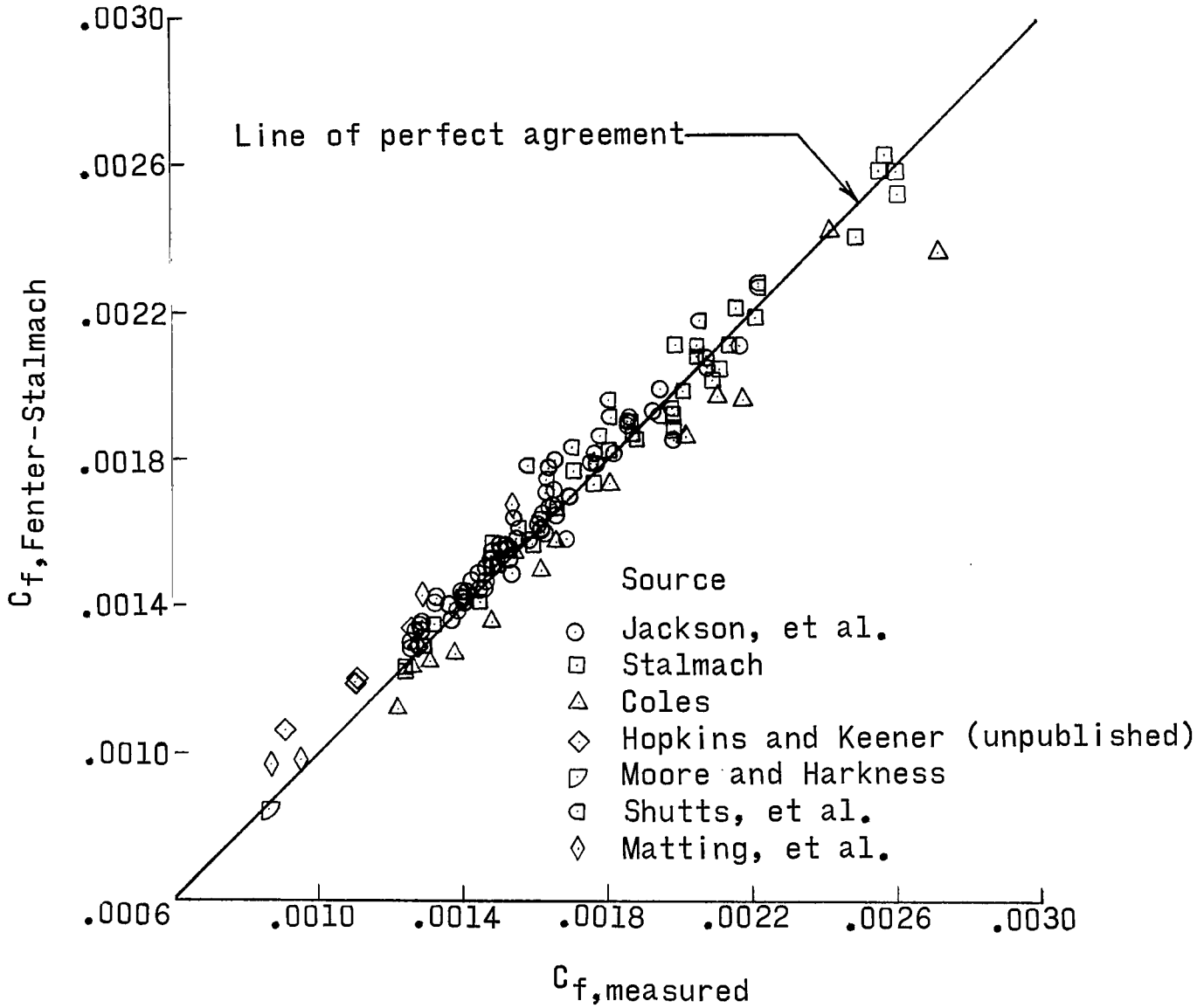

Figure 4.- Comparison between calculated and measured skin friction. Fenter-Stalmach equation.

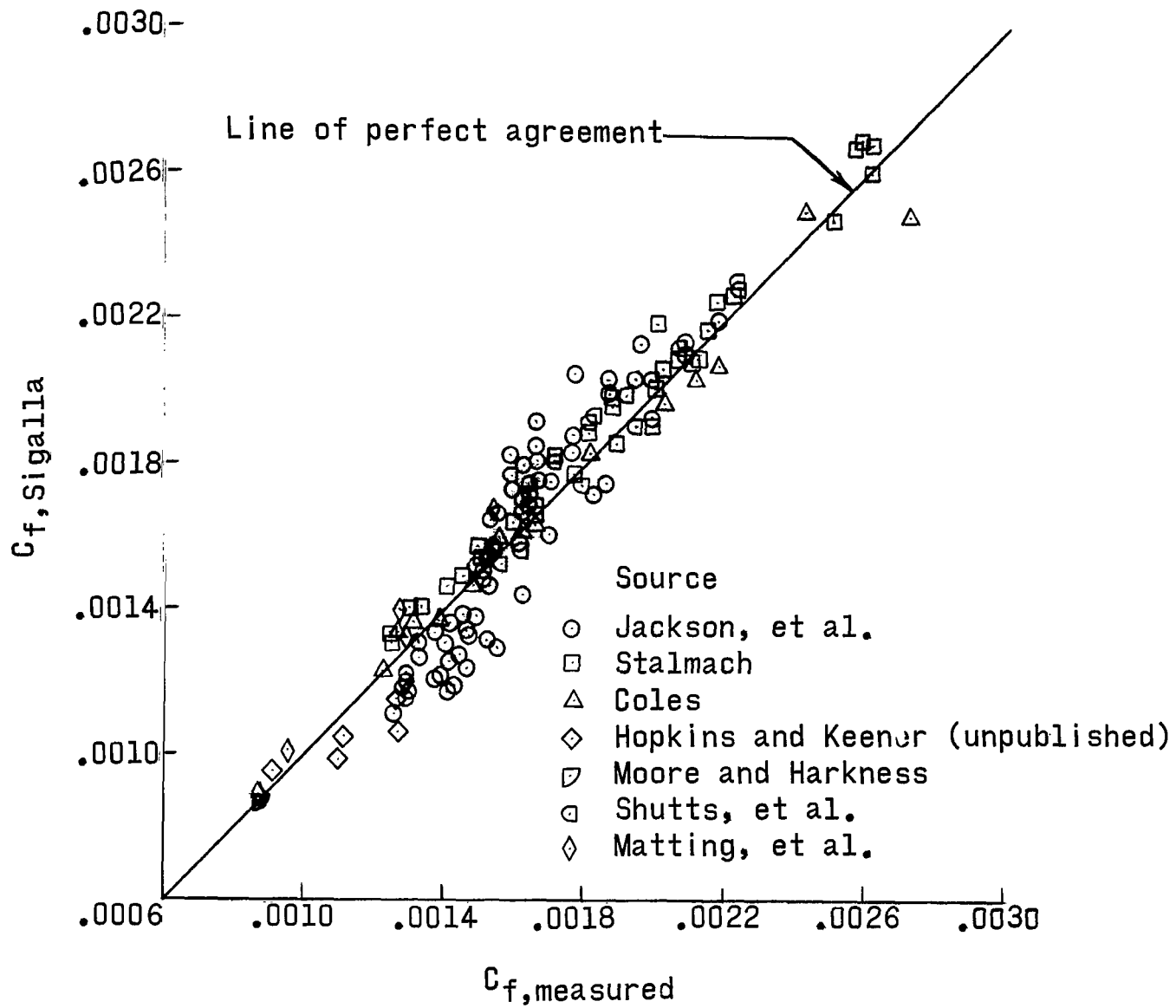

Figure 5.- Comparison between calculated and measured skin friction. Sigalla equation.

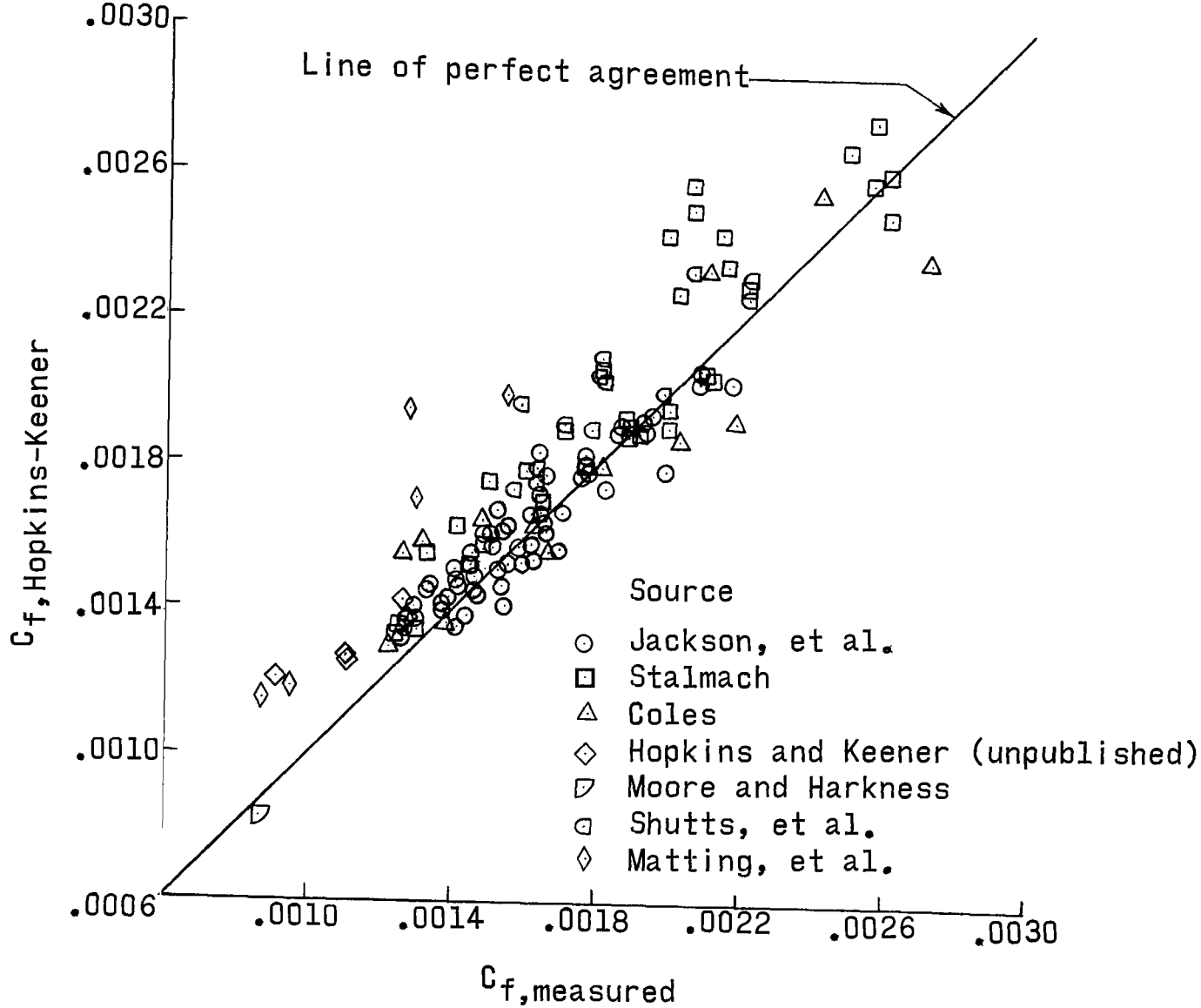

Figure 6.- Comparison between calculated and measured skin friction. Hopkins-Keener equation.

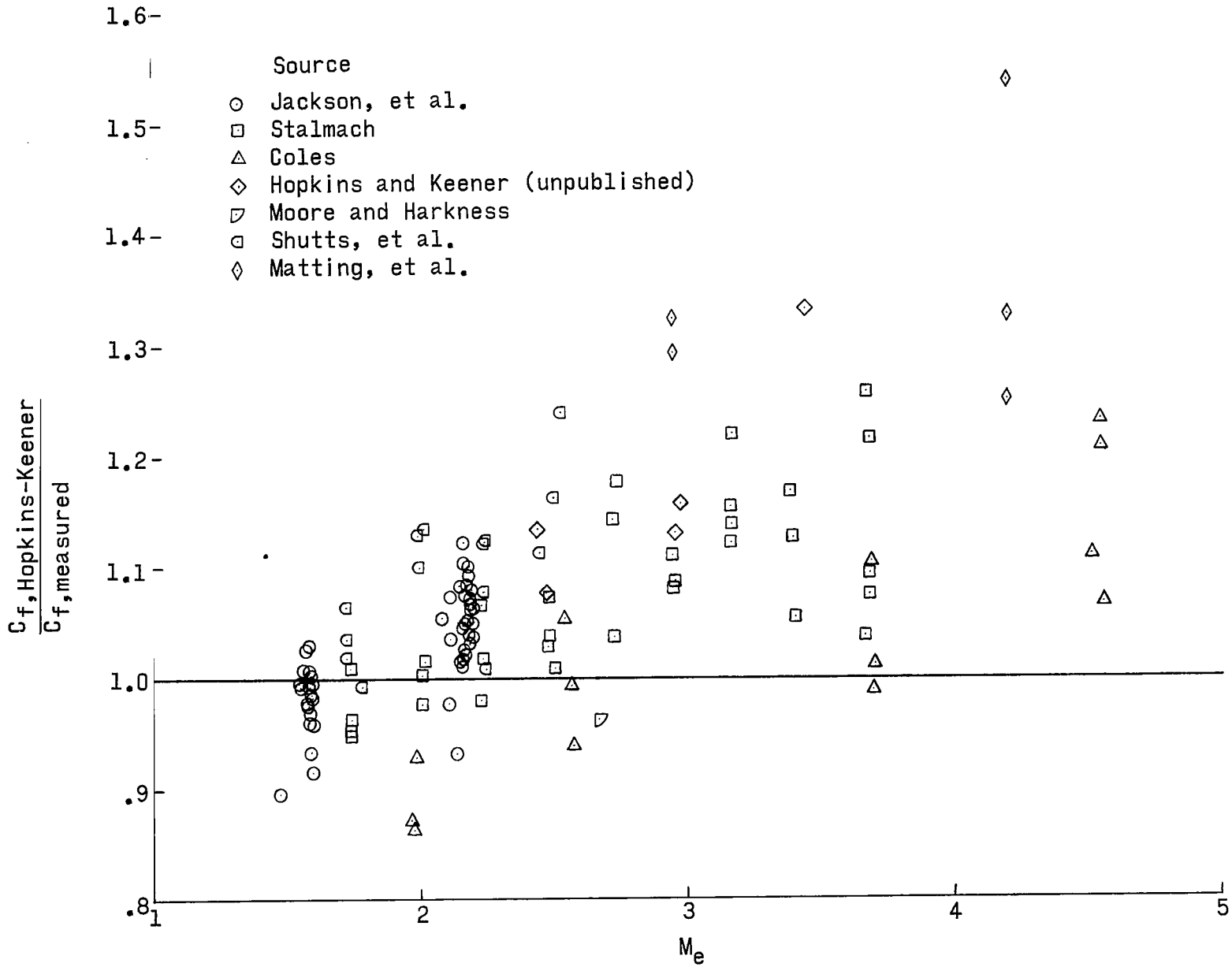

Figure 7.- Effect of Mach number on calculated skin friction. Hopkins-Keener equation.

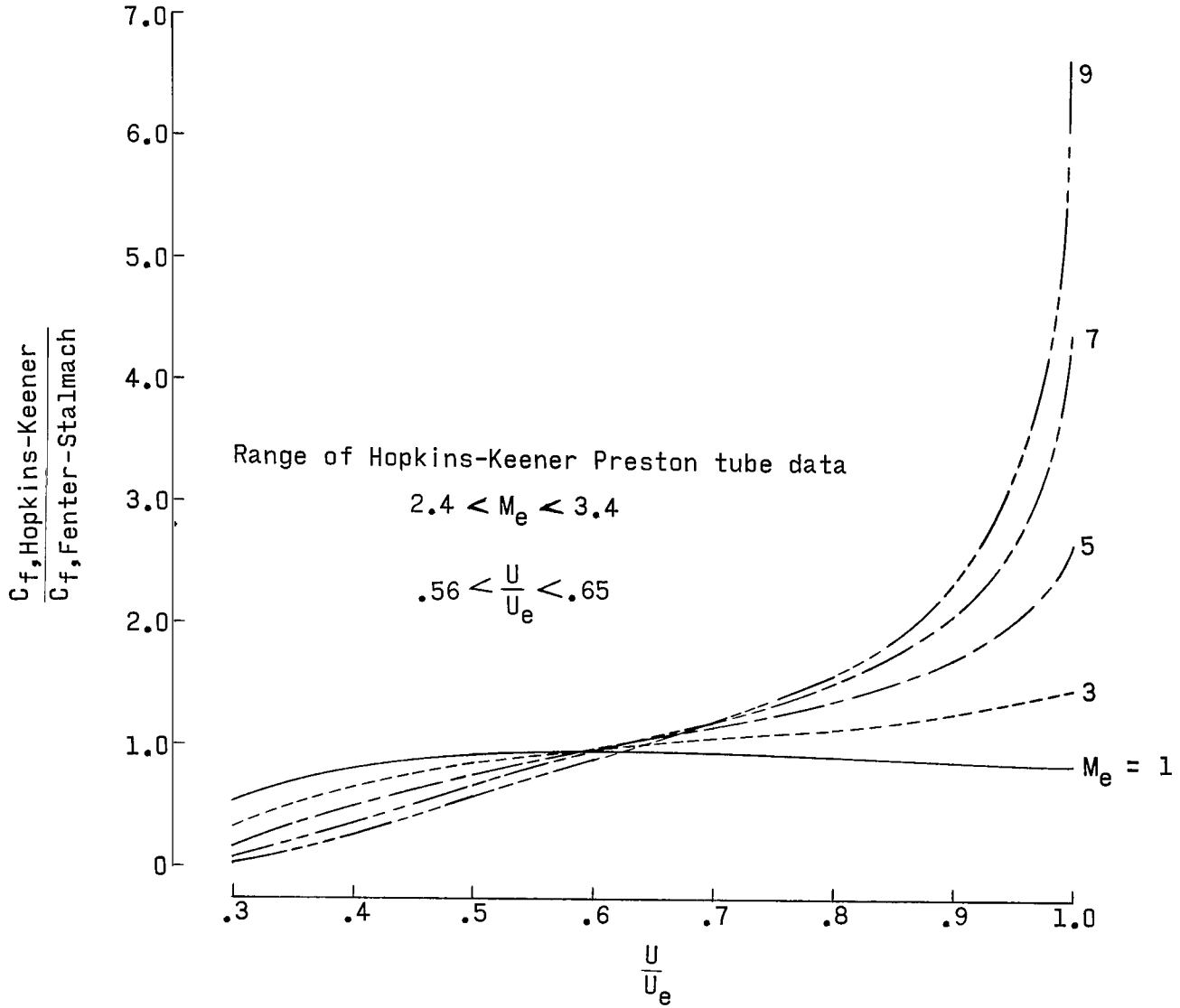

Figure 8.- Comparison between Hopkins-Keener and Fenter-Stalmach Preston tube calibrations. $\frac{U}{U_e} = \left(\frac{y}{\delta}\right)^{1/7}$; $R = 0.197 \times 10^6/\text{cm}$; $T_t = 316^0$ K; $\delta = 2.54$ cm; $\frac{T_w}{T_{aw}} = 1.0$.

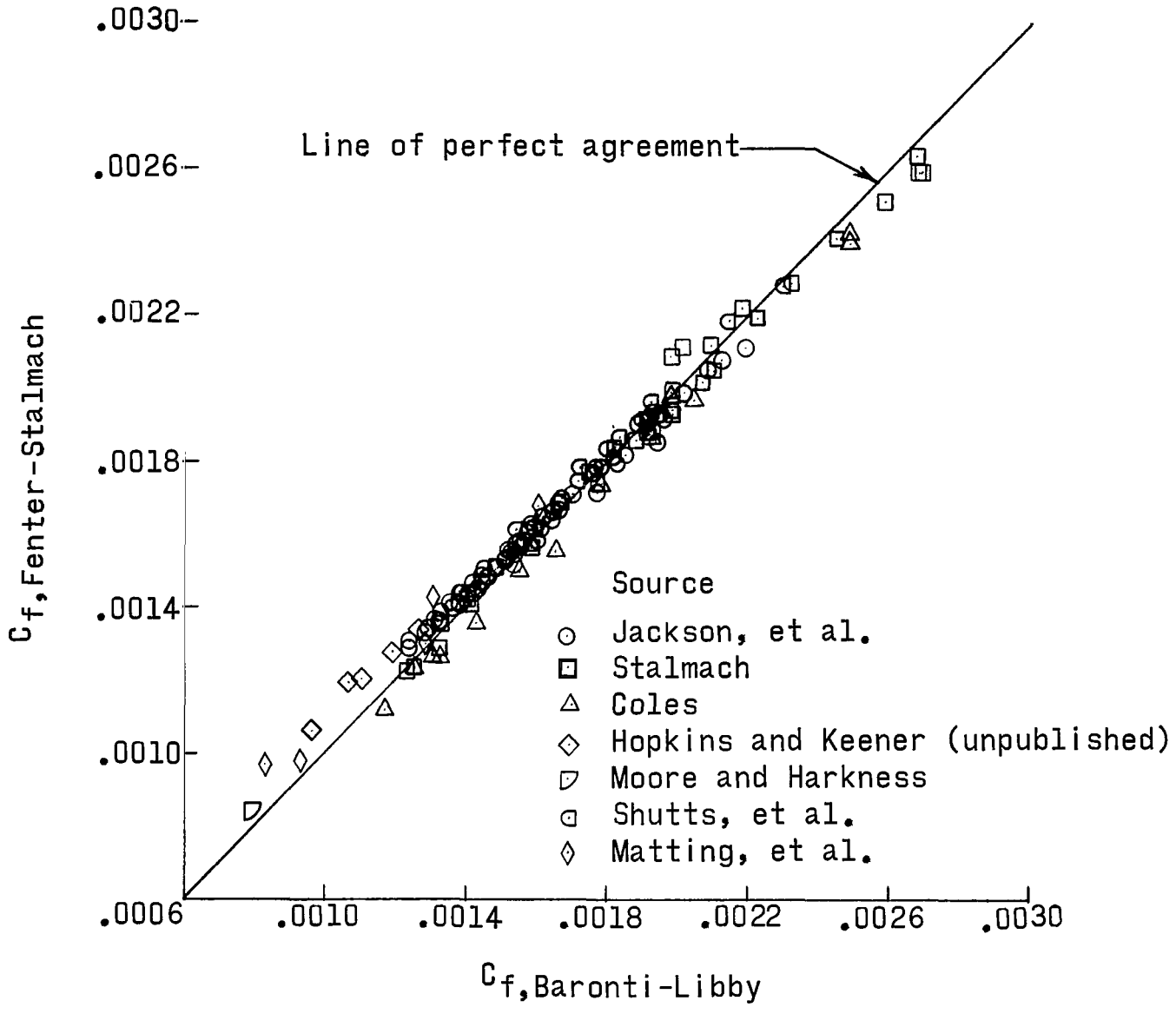

Figure 9.- Comparison between Fenter-Stalmach and Baronti-Libby calculations for adiabatic profiles.

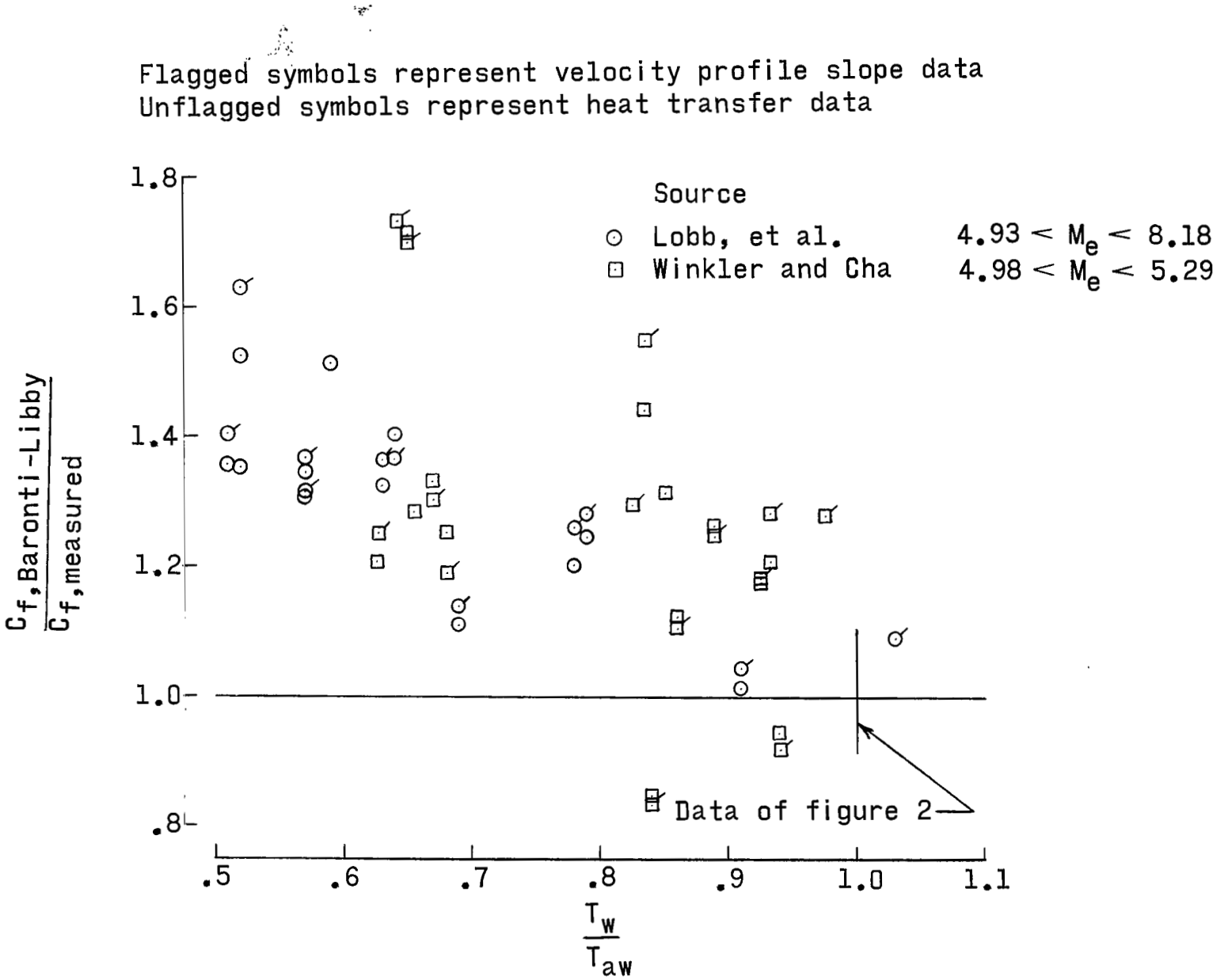

Figure 10.- Effect of wall temperature on skin friction calculated by Baronti-Libby method.

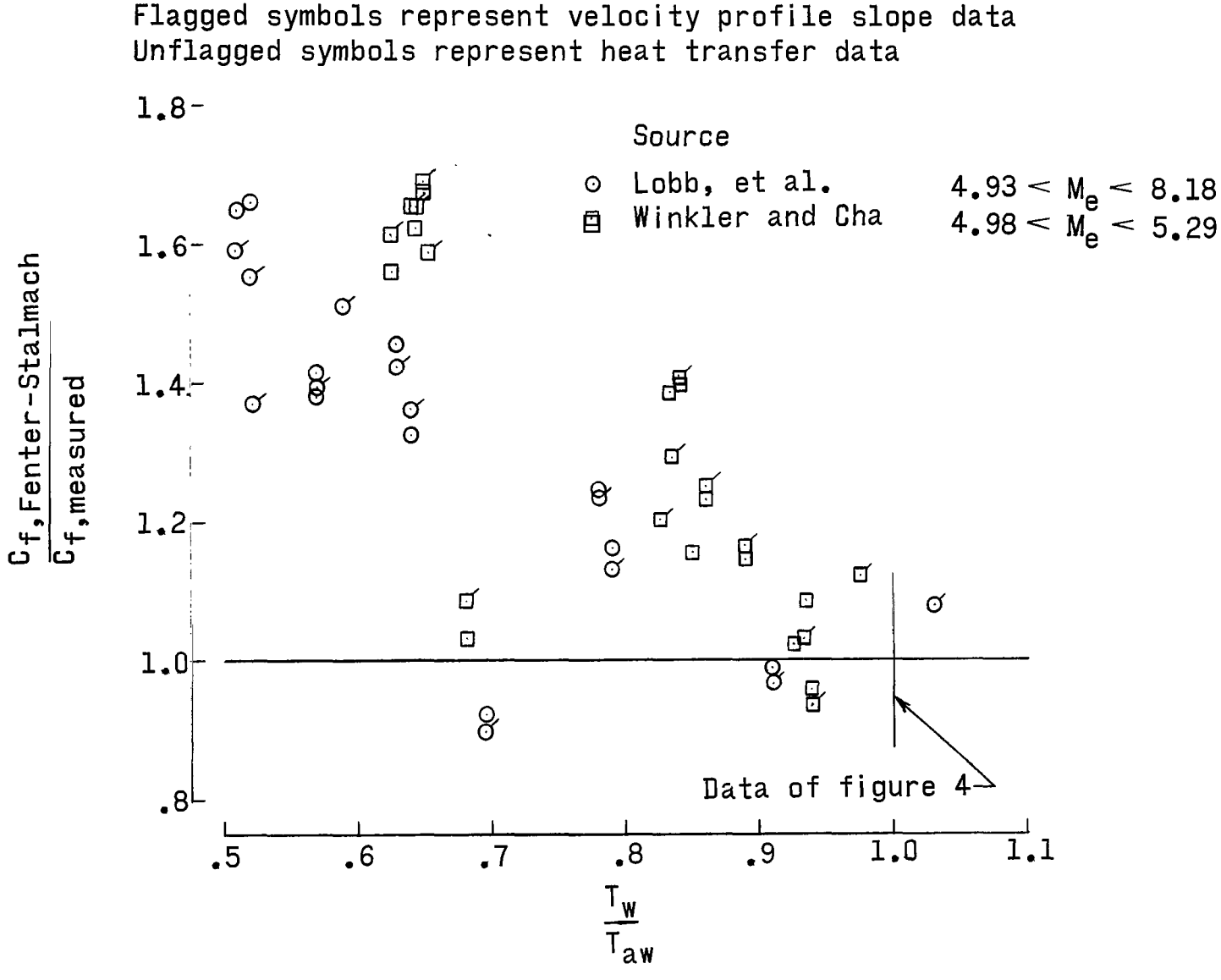

Figure 11.- Effect of wall temperature on skin friction calculated from Fenter-Stalmach equation.

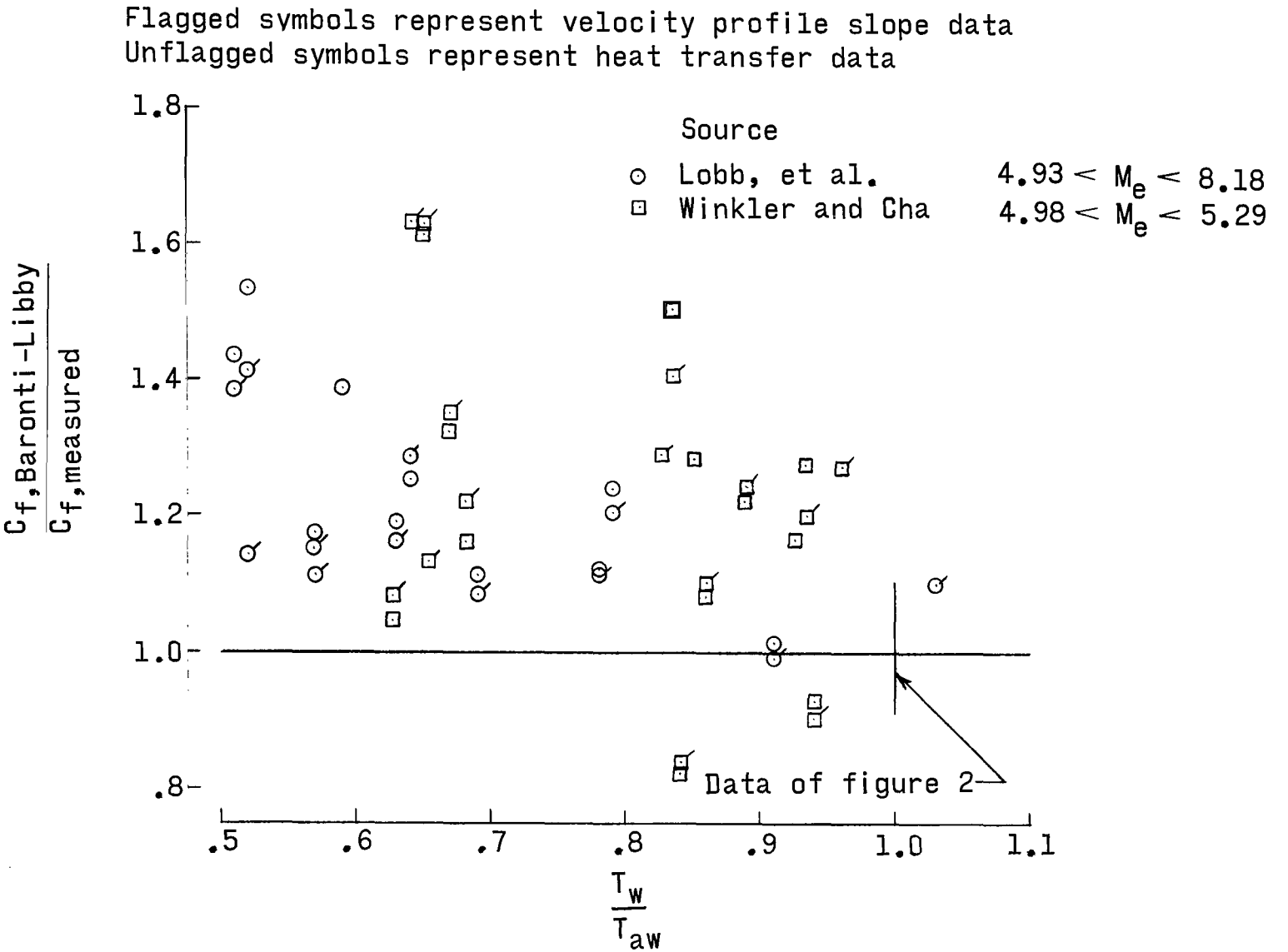

Figure 12.- Effect of wall temperature on skin friction calculated from adiabatic Baronti-Libby equations.

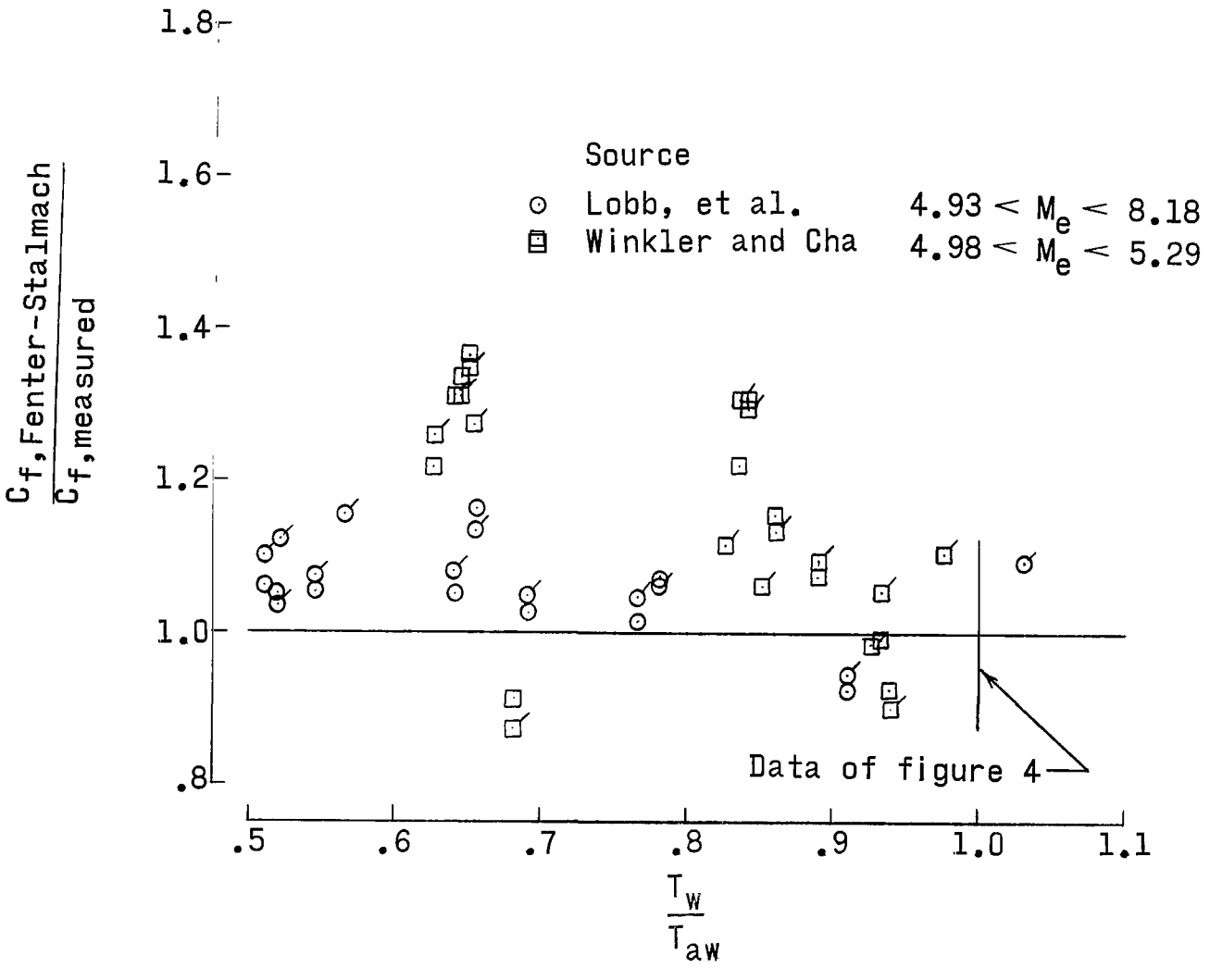

Figure 13.- Effect of wall temperature on skin friction calculated from adiabatic Fenter-Stalmach equation.

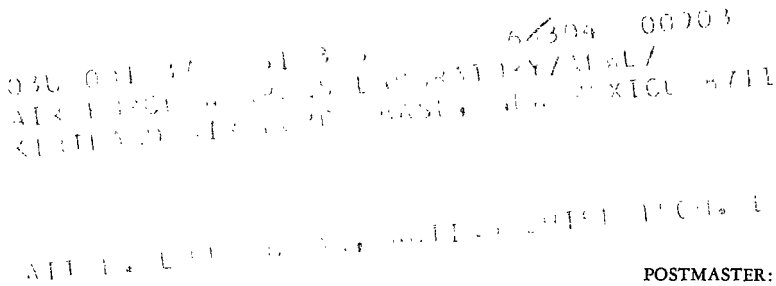

"The aeronautical and space activities of the United States shall be conducted so as to contribute . . . to the expansion of human knowledge of phenomena in the atmosphere and space. The Administration shall provide for the widest practicable and appropriate dissemination of information concerning its activities and the results thereof."

—NATIONAL AERONAUTICS AND SPACE ACT OF 1958

NASA SCIENTIFIC AND TECHNICAL PUBLICATIONS

TECHNICAL REPORTS: Scientific and technical information considered important, complete, and a lasting contribution to existing knowledge.

TECHNICAL NOTES: Information less broad in scope but nevertheless of importance as a contribution to existing knowledge.

TECHNICAL MEMORANDUMS: Information receiving limited distribution because of preliminary data, security classification, or other reasons.

CONTRACTOR REPORTS: Scientific and technical information generated under a NASA contract or grant and considered an important contribution to existing knowledge.

TECHNICAL TRANSLATIONS: Information published in a foreign language considered to merit NASA distribution in English.

SPECIAL PUBLICATIONS: Information derived from or of value to NASA activities. Publications include conference proceedings, monographs, data compilations, handbooks, sourcebooks, and special bibliographies.

TECHNOLOGY UTILIZATION PUBLICATIONS: Information on technology used by NASA that may be of particular interest in commercial and other non-aerospace applications. Publications include Tech Briefs, Technology Utilization Reports and Notes, and Technology Surveys.

Details on the availability of these publications may be obtained from:

SCIENTIFIC AND TECHNICAL INFORMATION DIVISION

NATIONAL AERONAUTICS AND SPACE ADMINISTRATION

Washington, D.C. 20546